



OPEN ACCESS

EDITED BY

Jeffrey W. Lynn,
National Institute of Standards and
Technology (NIST), United States

REVIEWED BY

Jianbao Zhao,
Canadian Light Source, Canada
Minghu Fang,
Zhejiang University, China

*CORRESPONDENCE

Gedefaw Mebratie Bogale,
✉ gedefawmebratie22@gmail.com

[†]These authors have contributed equally
to this work

RECEIVED 05 June 2023

ACCEPTED 20 November 2023

PUBLISHED 07 December 2023

CITATION

Bogale GM and Shiferaw DA (2023),
Theoretical study of the interplay of spin
density wave and superconductivity in
nickel substitution of the
strontium–iron–arsenide ($SrFe_{2-x}Ni_xAs_2$)
superconductor in a two-band model.
Front. Phys. 11:1235105.
doi: 10.3389/fphy.2023.1235105

COPYRIGHT

© 2023 Bogale and Shiferaw. This is an
open-access article distributed under the
terms of the [Creative Commons
Attribution License \(CC BY\)](https://creativecommons.org/licenses/by/4.0/). The use,
distribution or reproduction in other
forums is permitted, provided the original
author(s) and the copyright owner(s) are
credited and that the original publication
in this journal is cited, in accordance with
accepted academic practice. No use,
distribution or reproduction is permitted
which does not comply with these terms.

Theoretical study of the interplay of spin density wave and superconductivity in nickel substitution of the strontium–iron–arsenide ($SrFe_{2-x}Ni_xAs_2$) superconductor in a two-band model

Gedefaw Mebratie Bogale^{1*†} and Dagne Atnafu Shiferaw^{2†}

¹Department of Physics, Mekdela Amba University, Dessie, Ethiopia, ²Department of Physics, Dilla University, Dilla, Ethiopia

The main objective of this manuscript is to focus on the computational study of the interplay of spin density wave (SDW) and superconductivity using a two-band model for $SrFe_{2-x}Ni_xAs_2$. We derived mathematical statements for the superconducting critical temperature, SDW critical temperature, superconductivity order parameter, and the SDW order parameter using the Hamiltonian model and Green's function formalism for the $SrFe_{2-x}Ni_xAs_2$ superconductor. A mathematical expression for the dependence of transition temperatures on the SDW order parameter was obtained for $SrFe_{2-x}Ni_xAs_2$. Using these mathematical statements, transition temperatures versus the SDW order parameter phase diagrams were plotted to show the dependence of the SDW order parameter on transition temperatures. By merging these diagrams, we have depicted the intriguing possibility of the interplay of superconductivity and magnetism for the $SrFe_{2-x}Ni_xAs_2$ superconductor. Phase diagrams of temperature versus superconducting order parameters and the SDW order parameter were also plotted to show the dependence of order parameters on temperature for the $SrFe_{2-x}Ni_xAs_2$ superconductor.

KEYWORDS

superconductivity, superconducting transition temperature, superconducting order parameters, SDW transition temperature, SDW order parameter, magnetism

1 Introduction

Superconductivity was observed for the first time by a Dutch physicist Heike Kamerlingh Onnes. He found in 1911 that the electrical resistivity of *Hg* abruptly dropped to zero [1]. After 20 years of his discovery, in 1933, W. Meissner and his student R. Ochsenfeld found that the magnetic field is repelled by superconducting materials, called the Meissner effect [2]. This effect suggests a fundamental property of the superconducting state called perfect diamagnetism. In 1957, L. N. Cooper, J. Bardeen, and J. R. Schrieffer, the three American physicists, developed a quantum theory, called BCS theory, to elucidate the behaviour of superconducting materials at the microscopic level [3]. This theory claims that the formation

of quasiparticles termed Cooper pairs by the electrons in a material leads to superconductivity [4]. Cooper pairs are bosons and can aggregate in the same low-energy fundamental state (ground state energy), which is the superconducting state. It bases on a critical assumption that there is an attractive force between electrons. Electrons are fermions and are subject to the Pauli exclusion principle [5].

In the development of condensed matter physics, the discovery of high-transition temperature T_c superconductors marks a turning point. In 1979, the discovery of superconductivity in the heavy-fermion compound, $CeCu_2Si_2$ [6], came as a surprise because magnetic spin–spin interactions bind the superconducting charge carriers in pair and is highly unlikely by BCS theory [7]. The heavy-fermion system is the first class of unconventional superconductors. K. A. Muller and J. G. Bednorz discovered cuprates, the second class of high-temperature superconductors, in $La_{2-x}Ba_xCuO_4$ with $T_c = 35K$ [8]. Iron-based superconductors (FeSc), with $T_c = 26K$ in LaOFeAs, are the other family of high-temperature materials. They were identified by Hosono et al., in 2008 [9].

FeScs have various distinct systems that significantly enlarge the class of unconventional superconducting materials. Numerous FeSc systems with various compositions and crystal structure classes are found still now. Different systems are distinguished for convenience by the stoichiometric proportions of the chemical components of their parent molecules [10, 11]. The most common FeSc systems that use this nomenclature are 245, 1144, 42622, 12442, 1111, 111, 11, and 122 (for example, $Rb_2Fe_4Se_5$, $CsEuFe_4As_4$, $Sr_4V_2O_6Fe_2As_2$, $RbCa_2Fe_4As_4F_2$, $SmO_{1-x}F_xFeAs$, $NaFeAs$, $Fe_{1+y}Te_{1-x}Se_x$, and $SrFe_{2-x}Ni_xAs_2$) [12–16]. In the 245 FeSc system, $Rb_2Fe_4Se_5$, there is a unique phase separation phenomenon, unlike most other FeSc systems, and each phase separation has arrived from the competition between magnetic and superconducting ordering in the material [17, 18]. Despite having various structural variations, all FeSc systems have one thing in common: iron-based square-planar sheets [19]. FeSc systems contain iron-based layers, which are essential for their superconductivity, similar to copper oxide-based superconductors, in which oxygen—together with copper—creates the superconductivity layer [20].

According to theories, the parent materials of FeSc are semi-metallic, and the density of state close to Fermi's surface is primarily supplied by the iron 3d electrons (orbitals) and all five of the 3d orbitals cross Fermi's surface [21]. Just from the most experimental results and the band structure calculations, the results reveal three iron 3d orbitals (d_{xy} , d_{yz} , and d_{xz}) provide the primary contribution to the density of states near the Fermi level and they ruffle weakly in the z direction [22]. Two electron pockets are situated at the margin of the Brillouin zone (BZ) point, and two hole pockets are distributed evenly throughout the resultant Fermi surface. The weights of the three orbitals, ($d_{x^2-y^2}$, d_{yz} , and d_{xy}), are almost equal when doping is near optimum [23]. The two-orbital model and this idea of density of state will be used in this article's computations.

Within the two-orbital model, the electron Fermi pocket is close to the $(\pi, 0)$ point and is made up of the orbital d_{yz} , whereas the hole Fermi pocket around the $(0, 0)$ point is made up of a combination of d_{xz} and d_{yz} orbitals. The inter-band spin fluctuation resulting from this nesting is actually the particle hole scattering that occurs between the d_{xz} and d_{yz} orbitals since the component of the hole

Fermi pocket coupled by the nesting wave vector $(\pi, 0)$ is primarily of the d_{xz} orbital characteristic [24]. The amount of doping affects how the electrical band structure is shaped. In electron-doped materials, such as 122 Fe-based superconductor compounds, the Fermi surface has many quasi 2D warped cylinders centred Γ point around $(k = 0, 0)$ and M $(k = \pi, \pi)$, as well as a potential quasi 3D pocket close to $k_z = \pi$. For electron-doped 122 systems such as $SrFe_{2-x}Ni_xAs_2$, the electron Fermi pocket expands as the doping level rises, while the hole Fermi pocket contracts until at the strongly doped level, where the hole Fermi pocket eventually disappears. The opposite is true for hole-doped systems [20].

The spin density wave (SDW) state, first proposed by Overhauser in 1962, is where the electronic spin density forms a static wave and makes it a type of anti-ferromagnetic state [25]. It happens in anisotropic low-dimensional compounds at low temperatures. The spin and SDW are coupled. It describes the spin density periodic modulation specified by the Fermi wave number [26]. There is no net magnetization over the entire volume with the density varying perpendicularly as a function of position. When delocalized or itinerant electrons, rather than localized electrons, are responsible for the spatial spin density modulation and the SDW transition takes place. Its origin can be electron–hole pairing or finite wave vector singularities of the magnetic susceptibility [27]. It is Fermi surface nesting that is responsible for SDW stabilization. Nesting of the Fermi surface and SDW are observed in $SrFe_2As_2$ [28]. Although the SDW transition leads to the establishment of AFM order, which causes the moment of the iron atoms to become still along the longer axis in the orthorhombic phase, and the orthorhombic deformation of the crystal lattice transforms the structure of the crystal from the tetragonal to the orthorhombic phase [29].

The FeAs tetrahedral layers are present in the parent compounds of the 122 iron pnictide superconductors, which also show structural transitions from tetragonal to orthorhombic and from paramagnetic (PM) to anti-ferromagnetic (AFM) structures [30]. It has been demonstrated that the AFM orthorhombic phase is the parent phase of the pnictide superconductor that produces the SDW state, which can be suppressed to produce superconductivity by applying pressure or through chemical doping. It has been demonstrated that the parent pnictide compound structural and magnetic phase transitions are crucial in causing superconductivity [31]. The structural and magnetic transitions in our compound $SrFe_{2-x}Ni_xAs_2$ occur simultaneously at $T_S = T_N \approx 205K$ [25, 32, 33]. The transition can be tracked to the concentration $x = 0.15$, where T_S (T_N) $\approx 40K$ [34], but T_S (T_N) disappears for $x > 0.15$ or it is not observed in $x = 0.16$, which leads to maximum T_c [35]. In the concentration range $0.10 \leq x \leq 0.22$, superconductivity is observed for $SrFe_{2-x}Ni_xAs_2$. As the doping level [x in $SrFe_{2-x}Ni_xAs_2$] increases, the hole Fermi pocket continuously shrinks, whereas the electron pocket becomes larger, and the hole pocket finally vanishes in the heavily doped region, where superconductivity also disappears. Magnetic transition is strongly coupled with the structural distortion. Superconductivity has been demonstrated that the result from the suppression of the AFM state of $SrFe_2As_2$ by nickel substitution. The suppression of the long-range magnetic ordering and the sudden appearance of the Sc state at the same time are correlated, which suggests that the spin fluctuation of the Fe moments is crucial in creating the superconductive state [36]. The

closeness of structural and magnetic transitions suggests that spin and lattice coupling has occurred. Lower symmetry enables the spins to organise and, therefore, reduce magnetic frustrations, which is assumed to be the source of the crystal deformation [37].

FebSc are so interesting because they show the coexistence of superconductivity and magnetism. Therefore, they show a lot of promise for applications. They are desirable for electrical power stations and magnetic applications (Maglev trains) because they have a substantially larger critical magnetic field than cuprates or heavy fermions and high isotropic critical currents. Superconductivity shows potential to have a significant impact on our community and the realisation of a world with minimal carbon emissions [38]. In this article, the researchers study the coexistence of superconductivity and SDW in a two-band model for the iron-based superconductor $SrFe_{2-x}Ni_xAs_2$ by using Green's function formalism.

Based on the concepts of electronic structure, this article is investigated theoretically on the coexistence of superconductivity and SDW in nickel substitution of the strontium-iron-arsenide ($SrFe_{2-x}Ni_xAs_2$) superconductor in a two-band model. By considering a two-band model of Hamiltonian and using the double-time temperature-dependent Green's function formalism methodology, researchers tried to discover the mathematical statements for the critical temperatures (T_c and T_M) and order parameters (Δ_{Sc} and M).

2 Mathematical formulation of the problem

We explore a two-band model that encapsulates the fundamental physics of the multi-band unconventional superconducting state and SDW order and has a self-consistent solution in order to investigate the coexistence of superconductivity and SDW. The mean-field model Hamiltonian for the interplay of SDW and superconductivity in our compound in a two-band model (d_{yz} , say s and d_{xz} , say d) can be expressed as [39–41]

$$\begin{aligned} \hat{H} = & \sum_{k,\sigma} \epsilon_s(k) \hat{s}_{k,\sigma}^\dagger \hat{s}_{k,\sigma} + \sum_{k,\sigma} \epsilon_d(k) \hat{d}_{k,\sigma}^\dagger \hat{d}_{k,\sigma} - \Delta_{Sc}^s \sum_k (\hat{s}_{k\uparrow}^\dagger \hat{s}_{-k\downarrow}^\dagger + \hat{s}_{-k\downarrow} \hat{s}_{k\uparrow}) \\ & - \Delta_{Sc}^d \sum_k (\hat{d}_{k\uparrow}^\dagger \hat{d}_{-k\downarrow}^\dagger + \hat{d}_{-k\downarrow} \hat{d}_{k\uparrow}) - \Delta_{Sc}^{sd} \sum_k (\hat{s}_{k\uparrow}^\dagger \hat{s}_{-k\downarrow}^\dagger + \hat{d}_{-k\downarrow} \hat{d}_{k\uparrow}) \\ & - \Delta_{Sc}^{sd} \sum_k (\hat{d}_{k\uparrow}^\dagger \hat{d}_{-k\downarrow}^\dagger + \hat{s}_{-k\downarrow} \hat{s}_{k\uparrow}) \\ & - M \sum_k (\hat{s}_{(k+p)\uparrow}^\dagger \hat{d}_{k\uparrow}^\dagger + \hat{d}_{(k+p)\uparrow}^\dagger \hat{s}_{k\uparrow}^\dagger), \end{aligned} \tag{1}$$

where the first term indicates the energy of conduction electrons in the s -band. The second term indicates the energy of conduction electrons in the d -band. The third and fourth terms are the energies involving superconductivity due to the intra-band interactions at the s - and d -bands, respectively. The fifth and sixth terms are the energies involving superconductivity due to the inter-band interaction between bands s and d . The last term is the mean-field Hamiltonian which describes the magnetic interactions. $\epsilon_s(k)$ and $\epsilon_d(k)$ are energies of an electron measured with respect to the Fermi energy in s and d bands, respectively. $\hat{s}_{k\uparrow}^\dagger$ ($\hat{s}_{-k\downarrow}^\dagger$) are the creation (annihilation) operators in the s -intra-band interaction having the wave number k ($-k$) and spin \uparrow (\downarrow), respectively. $\hat{d}_{k\uparrow}^\dagger$ ($\hat{d}_{-k\downarrow}^\dagger$) are the creation (annihilation) operators in the d -intra-

band interaction having the wave number k ($-k$) and spin \uparrow (\downarrow), respectively. $\hat{s}_{(k+p)\uparrow}^\dagger$ ($\hat{d}_{(k+p)\uparrow}^\dagger$) are the operators which create fermions with momentum $(k + p)$ in the s (d) band interaction, respectively.

Δ_{Sc}^s is the superconducting order parameter (mean field) due to the intra-band interactions within the s band and is given by

$$\Delta_{Sc}^s = \sum_k U_s \ll (\hat{s}_{k\uparrow}^\dagger, \hat{s}_{-k\downarrow}^\dagger) \gg, \tag{2}$$

where U_s is the intra-band interaction potential in the s -band.

Δ_{Sc}^d is the superconducting order parameter (mean-field) due to the intra-band interactions within the d -band and is given by

$$\Delta_{Sc}^d = \sum_k U_d \ll (\hat{d}_{k\uparrow}^\dagger, \hat{d}_{-k\downarrow}^\dagger) \gg, \tag{3}$$

where U_d is the intra-band interaction potential in the d -band.

Δ_{Sc}^{sd} is the superconducting order parameter (mean-field) due to inter-band interactions between the s - band and d -bands, which is given by

$$\Delta_{Sc}^{sd} = \sum_k \frac{U_{sd}}{2} \left(\ll (\hat{s}_{k\uparrow}^\dagger, \hat{s}_{-k\downarrow}^\dagger) \gg + \ll (\hat{d}_{k\uparrow}^\dagger, \hat{d}_{-k\downarrow}^\dagger) \gg \right), \tag{4}$$

where U_{sd} is the inter-band interaction potential between the two bands.

The double-time temperature-dependent Green's function is used to find the equation of motion. This formalism is defined as

$$R_r(t-t') = \ll \hat{D}(t), \hat{E}(t') \gg = -i\theta(t-t') \langle [\hat{D}(t), \hat{E}(t')] \rangle. \tag{5}$$

$R_r(t-t')$ is boson operators' retarded response function. $\langle \dots \rangle$ and $\ll \dots \gg$ denote the thermodynamic average and abbreviated notation for the Green's function in the system, respectively. $\hat{D}(t)$ and $\hat{E}(t')$ are the Heisenberg notations of the field operators. They are expressed in terms of particle creation and annihilation operators or the quantized field function product. $\theta(t-t')$ represents the Heaviside step function and defined as $\theta(t-t') = 1$ if $t > t'$ and 0 if $t < t'$. $\hat{D}(t)$ can be written as $\hat{D}(t) = e^{i\hat{H}t} D(o) e^{-i\hat{H}t}$. $[\hat{D}(t), \hat{E}(t')]$ is the commutator or anti-commutator. This is described as $[\hat{D}(t), \hat{E}(t')] = \hat{D}(t)\hat{E}(t') - \zeta\hat{E}(t')\hat{D}(t)$, where $\zeta = 1$ for bosons and $\zeta = -1$ for fermions. To obtain the equations of motion, we differentiate Eq. 5 with time (t) as

$$\begin{aligned} \frac{d}{dt} R_r(t-t') &= -\frac{d}{dt} (i\theta(t-t') \langle [\hat{D}(t), \hat{E}(t')] \rangle) \\ \frac{d}{dt} R_r(t-t') &= -i \frac{d}{dt} \theta(t-t') \langle [\hat{D}(t), \hat{E}(t')] \rangle - i\theta(t-t') \\ &\frac{d}{dt} \langle [\hat{D}(t), \hat{E}(t')] \rangle, \end{aligned}$$

$$\begin{aligned} i\dot{R}_r(t-t') &= \frac{d}{dt} \theta(t-t') \langle [\hat{D}(t), \hat{E}(t')] \rangle \\ &+ \theta(t-t') \frac{d}{dt} \langle [\hat{D}(t), \hat{E}(t')] \rangle. \end{aligned} \tag{6}$$

The Dirac's delta function $\delta(t-t')$ is related to the Heaviside step function as

$$\theta(t-t') = \int_{-\infty}^t \delta(t-t'). \tag{7}$$

This implies the following:

$$\frac{d}{dt} \theta(t-t') = \delta(t-t'). \tag{8}$$

Now let us introduce the Heisenberg equations of motion as

$$\frac{d}{dt} \hat{D}(t) = [\hat{D}(t), \hat{H}]. \tag{9}$$

Substituting Eq. 8 and Eq. 9 into Eq. 6, we have the following:

$$i\dot{R}_r(t-t') = \delta(t-t') \langle [\hat{D}(t), \hat{E}(t')] \rangle + \ll [\hat{D}(t), \hat{H}], \hat{E}(t') \gg. \tag{10}$$

Let $R_r(\omega)$ be the Fourier transform of $R_r(t-t')$, which will be given by

$$R_r(t-t') = \int_{-\infty}^{\infty} R_r(\omega) e^{-i\omega(t-t')} d\omega. \tag{11}$$

The inverse Fourier transform is

$$R_r(\omega) = \frac{1}{2\pi} \int_{-\infty}^{\infty} R_r(t-t') e^{-i\omega(t-t')} d(t-t'). \tag{12}$$

The first-order derivative of Eq. 11 with time will be

$$i\dot{R}_r(t-t') = -i\omega \int_{-\infty}^{\infty} R_r(\omega) e^{-i\omega(t-t')} d\omega. \tag{13}$$

The Dirac delta function will be defined as

$$\delta(t-t') = \frac{1}{2\pi} \int_{-\infty}^{\infty} e^{-i\omega(t-t')} d\omega. \tag{14}$$

Substituting Eqs 13, 14 into Eq. 10, we have

$$\omega R_r(\omega) = \langle [\hat{D}(t), \hat{E}(t')] \rangle + \ll [\hat{D}(t), \hat{H}], \hat{E}(t') \gg. \tag{15}$$

Last but not the least, the formalism for the double-time temperature-dependent Green's function is

$$\omega \ll \hat{D}(t), \hat{E}(t') \gg = \langle [\hat{D}(t), \hat{E}(t')] \rangle + \ll [\hat{D}(t), \hat{H}], \hat{E}(t') \gg. \tag{16}$$

Here, $\ll \hat{D}(t), \hat{E}(t') \gg$ denotes the Fourier transform of Green's function involving the operators $\hat{D}(t)$ and $\hat{E}(t')$. We will apply the anti-commutation relation $[\hat{s}_{k\sigma}^\dagger, \hat{s}_{k\sigma'}^\dagger] = [\hat{s}_{k\sigma}, \hat{s}_{k\sigma'}] = 0$ and $[\hat{s}_{k\sigma}^\dagger, \hat{s}_{k\sigma'}] = \delta_{kk'} \delta_{\sigma\sigma'}$ to solve the equation of motion, where $\delta_{kk'} = \begin{cases} 1, & \text{if } k = k' \\ 0, & \text{otherwise} \end{cases}$ and $\delta_{\sigma\sigma'} = \begin{cases} 1, & \sigma = \sigma' \\ 0, & \text{otherwise} \end{cases}$

For simplification, Eq. 1 can be written as

$$\hat{H} = \hat{H}_s + \hat{H}_d + \hat{H}_{sd} + \hat{H}_M, \tag{17}$$

where

$$\hat{H}_s = \sum_{k,\sigma} \varepsilon_s(k) \hat{s}_{k,\sigma}^\dagger \hat{s}_{k,\sigma} - \Delta_{Sc}^s \sum_k (\hat{s}_{k\uparrow}^\dagger \hat{s}_{-k\downarrow}^\dagger + \hat{s}_{-k\downarrow} \hat{s}_{k\uparrow}).$$

This is s intra-band interaction's mean-field Hamiltonian.

$$\hat{H}_d = \sum_{k,\sigma} \varepsilon_s(k) \hat{d}_{k,\sigma}^\dagger \hat{d}_{k,\sigma} - \Delta_{Sc}^d \sum_k (\hat{d}_{k\uparrow}^\dagger \hat{d}_{-k\downarrow}^\dagger + \hat{d}_{-k\downarrow} \hat{d}_{k\uparrow}).$$

This is d intra-band interaction's mean-field Hamiltonian.

$$\hat{H}_{sd} = -\Delta_{Sc}^{sd} \sum_k (\hat{s}_{k\uparrow}^\dagger \hat{s}_{-k\downarrow}^\dagger + \hat{d}_{-k\downarrow} \hat{d}_{k\uparrow}) - \Delta_{Sc}^{sd} \sum_k (\hat{d}_{k\uparrow}^\dagger \hat{d}_{-k\downarrow}^\dagger + \hat{s}_{-k\downarrow} \hat{s}_{k\uparrow}).$$

This is the mean-field Hamiltonian in the inter-band interaction

$$\hat{H}_M = -M \sum_k (\hat{s}_{(k+p)\uparrow}^\dagger, \hat{d}_{k\uparrow} + \hat{d}_{(k+p)\uparrow}^\dagger, \hat{s}_{k\uparrow}).$$

This is the mean-field Hamiltonian due to the magnetic interaction of conduction electrons.

2.1 Superconducting order parameters in the pure superconducting region

2.1.1 Δ_{Sc}^s due to intra-band interactions within the s-band

To describe the superconducting order parameter due to the intra-band interaction within the s-band in the pure superconducting region, one can use the equation of motion for the correlation $\ll \hat{s}_{k\uparrow}^\dagger, \hat{s}_{-k\downarrow}^\dagger \gg$, and the following equation can be written:

$$\omega \ll \hat{s}_{k\uparrow}^\dagger, \hat{s}_{-k\downarrow}^\dagger \gg = \langle [\hat{s}_{k\uparrow}^\dagger, \hat{s}_{-k\downarrow}^\dagger] \rangle + \ll \hat{s}_{k\uparrow}^\dagger, \hat{H} \rangle, \hat{s}_{-k\downarrow}^\dagger \gg, \tag{18}$$

$$\omega \ll \hat{s}_{k\uparrow}^\dagger, \hat{s}_{-k\downarrow}^\dagger \gg = 0 + \ll [\hat{s}_{k\uparrow}^\dagger, \hat{H}_s + \hat{H}_d + \hat{H}_{sd} + \hat{H}_M], \hat{s}_{-k\downarrow}^\dagger \gg. \tag{19}$$

The commutation relations in Eq. 19 can be solved as follows: $[\hat{s}_{k\uparrow}^\dagger, \hat{H}_s] = [\hat{s}_{k\uparrow}^\dagger, \sum_{k,\sigma} \varepsilon_s(k) \hat{s}_{k,\sigma}^\dagger \hat{s}_{k,\sigma} - \Delta_{Sc}^s \sum_k (\hat{s}_{k\uparrow}^\dagger \hat{s}_{-k\downarrow}^\dagger + \hat{s}_{-k\downarrow} \hat{s}_{k\uparrow})]$ $[\hat{s}_{k\uparrow}^\dagger, \hat{H}_s] = \sum_{k,\sigma} \varepsilon_s(k) [\hat{s}_{k\uparrow}^\dagger, \hat{s}_{k,\sigma}^\dagger \hat{s}_{k,\sigma}] - \Delta_{Sc}^s \sum_k ([\hat{s}_{k\uparrow}^\dagger, \hat{s}_{k\uparrow}^\dagger \hat{s}_{-k\downarrow}^\dagger] + [\hat{s}_{k\uparrow}^\dagger, \hat{s}_{-k\downarrow} \hat{s}_{k\uparrow}])$ $[\hat{s}_{k\uparrow}^\dagger, \hat{H}_s] = \sum_{k,\sigma} \varepsilon_s(k) ([\hat{s}_{k\uparrow}^\dagger, \hat{s}_{k,\sigma}^\dagger] \hat{s}_{k,\sigma} - \hat{s}_{k,\sigma}^\dagger [\hat{s}_{k\uparrow}^\dagger, \hat{s}_{k,\sigma}]) - \Delta_{Sc}^s \sum_k ([\hat{s}_{k\uparrow}^\dagger, \hat{s}_{-k\downarrow}^\dagger] \hat{s}_{-k\downarrow} - \hat{s}_{-k\downarrow}^\dagger [\hat{s}_{k\uparrow}^\dagger, \hat{s}_{-k\downarrow}^\dagger]) + [\hat{s}_{k\uparrow}^\dagger, \hat{s}_{-k\downarrow} \hat{s}_{k\uparrow}]$

$$[\hat{s}_{k\uparrow}^\dagger, \hat{H}_s] = -\varepsilon_s(k) \hat{s}_{k\uparrow}^\dagger + \Delta_{Sc}^s \hat{s}_{-k\downarrow}. \tag{20}$$

$[\hat{s}_{k\uparrow}^\dagger, \hat{H}_d] = [\hat{s}_{k\uparrow}^\dagger, \sum_{k,\sigma} \varepsilon_s(k) \hat{d}_{k,\sigma}^\dagger \hat{d}_{k,\sigma} - \Delta_{Sc}^d \sum_k (\hat{d}_{k\uparrow}^\dagger \hat{d}_{-k\downarrow}^\dagger + \hat{d}_{-k\downarrow} \hat{d}_{k\uparrow})]$ $[\hat{s}_{k\uparrow}^\dagger, \hat{H}_d] = \sum_{k,\sigma} \varepsilon_s(k) ([\hat{s}_{k\uparrow}^\dagger, \hat{d}_{k,\sigma}^\dagger \hat{d}_{k,\sigma}] - \Delta_{Sc}^d \sum_k ([\hat{s}_{k\uparrow}^\dagger, \hat{d}_{k\uparrow}^\dagger \hat{d}_{-k\downarrow}^\dagger] + [\hat{s}_{k\uparrow}^\dagger, \hat{d}_{-k\downarrow} \hat{d}_{k\uparrow}])$ $[\hat{s}_{k\uparrow}^\dagger, \hat{H}_d] = \sum_{k,\sigma} \varepsilon_s(k) ([\hat{s}_{k\uparrow}^\dagger, \hat{d}_{k,\sigma}^\dagger] \hat{d}_{k,\sigma} - \hat{d}_{k,\sigma}^\dagger [\hat{s}_{k\uparrow}^\dagger, \hat{d}_{k,\sigma}]) - \Delta_{Sc}^d \sum_k ([\hat{s}_{k\uparrow}^\dagger, \hat{d}_{k\uparrow}^\dagger \hat{d}_{-k\downarrow}^\dagger] - \hat{d}_{k\uparrow}^\dagger [\hat{s}_{k\uparrow}^\dagger, \hat{d}_{-k\downarrow}^\dagger] + [\hat{s}_{k\uparrow}^\dagger, \hat{d}_{-k\downarrow} \hat{d}_{k\uparrow}] - \hat{d}_{-k\downarrow} [\hat{s}_{k\uparrow}^\dagger, \hat{d}_{k\uparrow}])$

$$[\hat{s}_{k\uparrow}^\dagger, \hat{H}_d] = 0. \tag{21}$$

$[\hat{s}_{k\uparrow}^\dagger, \hat{H}_{sd}] = [\hat{s}_{k\uparrow}^\dagger, -\Delta_{Sc}^{sd} \sum_k (\hat{s}_{k\uparrow}^\dagger \hat{s}_{-k\downarrow}^\dagger + \hat{d}_{-k\downarrow} \hat{d}_{k\uparrow}) - \Delta_{Sc}^{sd} \sum_k (\hat{d}_{k\uparrow}^\dagger \hat{d}_{-k\downarrow}^\dagger + \hat{s}_{-k\downarrow} \hat{s}_{k\uparrow})]$ $[\hat{s}_{k\uparrow}^\dagger, \hat{H}_{sd}] = -\Delta_{Sc}^{sd} \sum_k ([\hat{s}_{k\uparrow}^\dagger, \hat{d}_{k\uparrow}^\dagger \hat{d}_{-k\downarrow}^\dagger] + [\hat{s}_{k\uparrow}^\dagger, \hat{d}_{-k\downarrow} \hat{d}_{k\uparrow}]) - \Delta_{Sc}^{sd} \sum_k ([\hat{s}_{k\uparrow}^\dagger, \hat{s}_{-k\downarrow} \hat{s}_{k\uparrow}])$ $[\hat{s}_{k\uparrow}^\dagger, \hat{H}_{sd}] = -\Delta_{Sc}^{sd} \sum_k ([\hat{s}_{k\uparrow}^\dagger, \hat{d}_{k\uparrow}^\dagger] \hat{d}_{-k\downarrow}^\dagger + [\hat{s}_{k\uparrow}^\dagger, \hat{d}_{-k\downarrow} \hat{d}_{k\uparrow}]) - \Delta_{Sc}^{sd} \sum_k ([\hat{s}_{k\uparrow}^\dagger, \hat{s}_{-k\downarrow} \hat{s}_{k\uparrow}])$ $[\hat{s}_{k\uparrow}^\dagger, \hat{H}_{sd}] = -\Delta_{Sc}^{sd} \sum_k ([\hat{s}_{k\uparrow}^\dagger, \hat{d}_{k\uparrow}^\dagger] \hat{d}_{-k\downarrow}^\dagger - \hat{d}_{k\uparrow}^\dagger [\hat{s}_{k\uparrow}^\dagger, \hat{d}_{-k\downarrow}^\dagger] + [\hat{s}_{k\uparrow}^\dagger, \hat{d}_{-k\downarrow} \hat{d}_{k\uparrow}] - \hat{d}_{-k\downarrow} [\hat{s}_{k\uparrow}^\dagger, \hat{d}_{k\uparrow}]) - \Delta_{Sc}^{sd} \sum_k ([\hat{s}_{k\uparrow}^\dagger, \hat{s}_{-k\downarrow} \hat{s}_{k\uparrow}])$

$$[\hat{s}_{k\uparrow}^\dagger, \hat{H}_{sd}] = \Delta_{Sc}^{sd} \hat{s}_{-k\downarrow}. \tag{22}$$

$[\hat{s}_{k\uparrow}^\dagger, \hat{H}_M] = [\hat{s}_{k\uparrow}^\dagger, -M \sum_k (\hat{s}_{(k+p)\uparrow}^\dagger \hat{d}_{k\uparrow} + \hat{d}_{(k+p)\uparrow}^\dagger \hat{s}_{k\uparrow})]$ $[\hat{s}_{k\uparrow}^\dagger, \hat{H}_M] = M \sum_k ([\hat{s}_{k\uparrow}^\dagger, \hat{s}_{(k+p)\uparrow}^\dagger] \hat{d}_{k\uparrow} + [\hat{s}_{k\uparrow}^\dagger, \hat{d}_{(k+p)\uparrow}^\dagger] \hat{s}_{k\uparrow})$ $[\hat{s}_{k\uparrow}^\dagger, \hat{H}_M] = M \sum_k ([\hat{s}_{k\uparrow}^\dagger, \hat{s}_{(k+p)\uparrow}^\dagger] \hat{d}_{k\uparrow} - \hat{s}_{(k+p)\uparrow}^\dagger [\hat{s}_{k\uparrow}^\dagger, \hat{d}_{k\uparrow}] + [\hat{s}_{k\uparrow}^\dagger, \hat{d}_{(k+p)\uparrow}^\dagger] \hat{s}_{k\uparrow} - \hat{d}_{(k+p)\uparrow}^\dagger [\hat{s}_{k\uparrow}^\dagger, \hat{s}_{k\uparrow}])$

$$[\hat{s}_{k\uparrow}^\dagger, \hat{H}_M] = M \hat{d}_{(k+p)\uparrow}^\dagger. \tag{23}$$

Ignoring Eq. 23 and inserting Eq. 20 to Eq. 22 into Eq. 19, we get

$$\omega \ll \hat{s}_{k\uparrow}^\dagger, \hat{s}_{-k\downarrow}^\dagger \gg = \ll -\varepsilon_s(k) \hat{s}_{k\uparrow}^\dagger + \Delta_{Sc}^s \hat{s}_{-k\downarrow} + \Delta_{Sc}^{sd} \hat{s}_{-k\downarrow}, \hat{s}_{-k\downarrow}^\dagger \gg, \tag{24}$$

$$\omega \ll \hat{s}_{k\uparrow}^\dagger, \hat{s}_{-k\downarrow}^\dagger \gg = -\varepsilon_s(k) \ll \hat{s}_{k\uparrow}^\dagger, \hat{s}_{-k\downarrow}^\dagger \gg + \Delta_{Sc}^s \ll \hat{s}_{-k\downarrow}, \hat{s}_{-k\downarrow}^\dagger \gg + \Delta_{Sc}^{sd} \ll \hat{s}_{-k\downarrow}, \hat{s}_{-k\downarrow}^\dagger \gg, \tag{25}$$

$$(\omega + \varepsilon_s(k)) \ll \hat{s}_{k\uparrow}^\dagger, \hat{s}_{-k\downarrow}^\dagger \gg = (\Delta_{Sc}^s + \Delta_{Sc}^{sd}) \ll \hat{s}_{-k\downarrow}, \hat{s}_{-k\downarrow}^\dagger \gg, \tag{26}$$

$$\ll \hat{s}_{k\uparrow}^\dagger, \hat{s}_{-k\downarrow}^\dagger \gg = \frac{\Delta_{Sc}^s + \Delta_{Sc}^{sd}}{\omega + \varepsilon_s(k)} \ll \hat{s}_{-k\downarrow}, \hat{s}_{k\uparrow}^\dagger \gg. \quad (27)$$

The equation of motion for the homologous $\ll \hat{s}_{-k\downarrow}, \hat{s}_{k\uparrow}^\dagger \gg$ in Eq. 27 is described as

$$\omega \ll \hat{s}_{-k\downarrow}, \hat{s}_{k\uparrow}^\dagger \gg = \langle [\hat{s}_{-k\downarrow}, \hat{H}_s] \rangle + \ll [\hat{s}_{-k\downarrow}, \hat{H}] \gg, \quad (28)$$

$$\omega \ll \hat{s}_{-k\downarrow}, \hat{s}_{k\uparrow}^\dagger \gg = 1 + \ll [\hat{s}_{-k\downarrow}, \hat{H}_s + \hat{H}_d + \hat{H}_{sd}] \gg. \quad (29)$$

Evaluating the commutation relations in Eq. 29 which yields, $[\hat{s}_{-k\downarrow}, \hat{H}_s] = [\hat{s}_{-k\downarrow}, \sum_{k,\sigma} \varepsilon_s(k) \hat{s}_{k,\sigma} \sigma^\dagger \hat{s}_{k,\sigma} - \Delta_{Sc}^s \sum_k (\hat{s}_{k\uparrow}^\dagger \hat{s}_{-k\downarrow}^\dagger + \hat{s}_{-k\downarrow} \hat{s}_{k\uparrow}^\dagger)] [\hat{s}_{-k\downarrow}, \hat{H}_s] = \sum_{k,\sigma} \varepsilon_s(k) [\hat{s}_{-k\downarrow}, \hat{s}_{k,\sigma}^\dagger \hat{s}_{k,\sigma}] - \Delta_{Sc}^s \sum_k ([\hat{s}_{-k\downarrow}, \hat{s}_{k\uparrow}^\dagger \hat{s}_{-k\downarrow}^\dagger] + [\hat{s}_{-k\downarrow}, \hat{s}_{-k\downarrow} \hat{s}_{k\uparrow}^\dagger]) [\hat{s}_{-k\downarrow}, \hat{H}_d] = \sum_{k,\sigma} \varepsilon_s(k) ([\hat{s}_{-k\downarrow}, \hat{s}_{k,\sigma}^\dagger \hat{s}_{k,\sigma}] - \hat{s}_{k,\sigma}^\dagger [\hat{s}_{-k\downarrow}, \hat{s}_{k,\sigma} \sigma] - \Delta_{Sc}^s \sum_k ([\hat{s}_{-k\downarrow}, \hat{s}_{k\uparrow}^\dagger \hat{s}_{-k\downarrow}^\dagger] - \hat{s}_{k\uparrow}^\dagger [\hat{s}_{-k\downarrow}, \hat{s}_{k\uparrow}^\dagger] + [\hat{s}_{-k\downarrow}, \hat{s}_{-k\downarrow} \hat{s}_{k\uparrow}^\dagger] - \hat{s}_{-k\downarrow} [\hat{s}_{k\uparrow}^\dagger, \hat{s}_{-k\downarrow}]))$

$$[\hat{s}_{-k\downarrow}, \hat{H}_s] = \varepsilon_s(k) \hat{s}_{-k\downarrow} + \Delta_{Sc}^s \hat{s}_{k\uparrow}^\dagger. \quad (30)$$

$$[\hat{s}_{-k\downarrow}, \hat{H}_d] = [\hat{s}_{-k\downarrow}, \sum_{k,\sigma} \varepsilon_s(k) \hat{d}_{k,\sigma}^\dagger \hat{d}_k - \Delta_{Sc}^d \sum_k (\hat{d}_{k\uparrow}^\dagger \hat{d}_{-k\downarrow}^\dagger + \hat{d}_{-k\downarrow} \hat{d}_{k\uparrow}^\dagger)] [\hat{s}_{-k\downarrow}, \hat{H}_d] = \sum_{k,\sigma} \varepsilon_s(k) ([\hat{s}_{-k\downarrow}, \hat{d}_{k,\sigma}^\dagger \hat{d}_{k,\sigma}] - \Delta_{Sc}^d \sum_k ([\hat{s}_{-k\downarrow}, \hat{d}_{k\uparrow}^\dagger \hat{d}_{-k\downarrow}^\dagger] + [\hat{s}_{-k\downarrow}, \hat{d}_{-k\downarrow} \hat{d}_{k\uparrow}^\dagger]) [\hat{s}_{-k\downarrow}, \hat{H}_{sd}] = \sum_{k,\sigma} \varepsilon_s(k) ([\hat{s}_{-k\downarrow}, \hat{d}_{k,\sigma}^\dagger \hat{d}_{k,\sigma}] - \hat{d}_{k,\sigma}^\dagger [\hat{s}_{-k\downarrow}, \hat{d}_{k,\sigma}]) - \Delta_{Sc}^d \sum_k ([\hat{s}_{-k\downarrow}, \hat{d}_{k\uparrow}^\dagger \hat{d}_{-k\downarrow}^\dagger] - \hat{d}_{k\uparrow}^\dagger [\hat{s}_{-k\downarrow}, \hat{d}_{-k\downarrow}^\dagger] + [\hat{s}_{-k\downarrow}, \hat{d}_{-k\downarrow} \hat{d}_{k\uparrow}^\dagger] - \hat{d}_{-k\downarrow} [\hat{s}_{-k\downarrow}, \hat{d}_{k\uparrow}^\dagger])$$

$$[\hat{s}_{-k\downarrow}, \hat{H}_d] = 0. \quad (31)$$

$$[\hat{s}_{-k\downarrow}, \hat{H}_{sd}] = [\hat{s}_{-k\downarrow}, -\Delta_{Sc}^{sd} \sum_k (\hat{s}_{k\uparrow}^\dagger \hat{s}_{-k\downarrow}^\dagger + \hat{d}_{-k\downarrow} \hat{d}_{k\uparrow}^\dagger) - \Delta_{Sc}^{sd} \sum_k (\hat{d}_{k\uparrow}^\dagger \hat{d}_{-k\downarrow}^\dagger + \hat{s}_{-k\downarrow} \hat{s}_{k\uparrow}^\dagger)] [\hat{s}_{-k\downarrow}, \hat{H}_{sd}] = -\Delta_{Sc}^{sd} \sum_k ([\hat{s}_{-k\downarrow}, \hat{d}_{k\uparrow}^\dagger \hat{d}_{-k\downarrow}^\dagger] + [\hat{s}_{-k\downarrow}, \hat{d}_{-k\downarrow} \hat{d}_{k\uparrow}^\dagger]) - \Delta_{Sc}^{sd} \sum_k ([\hat{s}_{-k\downarrow}, \hat{d}_{k\uparrow}^\dagger \hat{d}_{-k\downarrow}^\dagger] + [\hat{s}_{-k\downarrow}, \hat{s}_{-k\downarrow} \hat{s}_{k\uparrow}^\dagger]) [\hat{s}_{-k\downarrow}, \hat{H}_{sd}] = -\Delta_{Sc}^{sd} \sum_k ([\hat{s}_{-k\downarrow}, \hat{d}_{k\uparrow}^\dagger \hat{d}_{-k\downarrow}^\dagger] - \hat{d}_{k\uparrow}^\dagger [\hat{s}_{-k\downarrow}, \hat{d}_{-k\downarrow}^\dagger] + [\hat{s}_{-k\downarrow}, \hat{d}_{-k\downarrow} \hat{d}_{k\uparrow}^\dagger] - \hat{d}_{-k\downarrow} [\hat{s}_{-k\downarrow}, \hat{d}_{k\uparrow}^\dagger]) - \Delta_{Sc}^{sd} \sum_k ([\hat{s}_{-k\downarrow}, \hat{d}_{k\uparrow}^\dagger \hat{d}_{-k\downarrow}^\dagger] - \hat{d}_{k\uparrow}^\dagger [\hat{s}_{-k\downarrow}, \hat{d}_{-k\downarrow}^\dagger] + [\hat{s}_{-k\downarrow}, \hat{d}_{-k\downarrow} \hat{d}_{k\uparrow}^\dagger] - \hat{d}_{-k\downarrow} [\hat{s}_{-k\downarrow}, \hat{d}_{k\uparrow}^\dagger])$$

$$[\hat{s}_{-k\downarrow}, \hat{H}_{sd}] = \Delta_{Sc}^{sd} \hat{s}_{k\uparrow}^\dagger. \quad (32)$$

Inserting Eq. 30 to Eq. 32 in Eq. 29, we get

$$\omega \ll \hat{s}_{-k\downarrow}, \hat{s}_{k\uparrow}^\dagger \gg = 1 + \ll \varepsilon_s(k) \hat{s}_{-k\downarrow} + \Delta_{Sc}^s \hat{s}_{k\uparrow}^\dagger + \Delta_{Sc}^{sd} \hat{s}_{k\uparrow}^\dagger, \hat{s}_{-k\downarrow}^\dagger \gg, \quad (33)$$

$$\omega \ll \hat{s}_{-k\downarrow}, \hat{s}_{k\uparrow}^\dagger \gg = 1 + \varepsilon_s(k) \ll \hat{s}_{-k\downarrow}, \hat{s}_{k\uparrow}^\dagger \gg + (\Delta_{Sc}^s + \Delta_{Sc}^{sd}) \ll \hat{s}_{k\uparrow}^\dagger, \hat{s}_{-k\downarrow}^\dagger \gg, \quad (34)$$

$$(\omega - \varepsilon_s(k)) \ll \hat{s}_{-k\downarrow}, \hat{s}_{k\uparrow}^\dagger \gg = 1 + (\Delta_{Sc}^s + \Delta_{Sc}^{sd}) \ll \hat{s}_{k\uparrow}^\dagger, \hat{s}_{-k\downarrow}^\dagger \gg, \quad (35)$$

$$\ll \hat{s}_{-k\downarrow}, \hat{s}_{k\uparrow}^\dagger \gg = \frac{1}{\omega - \varepsilon_s(k)} + \frac{\Delta_{Sc}^s + \Delta_{Sc}^{sd}}{\omega - \varepsilon_s(k)} \ll \hat{s}_{k\uparrow}^\dagger, \hat{s}_{-k\downarrow}^\dagger \gg. \quad (36)$$

Substituting Eq. 36 in Eq. 27, we get

$$\ll \hat{s}_{k\uparrow}^\dagger, \hat{s}_{-k\downarrow}^\dagger \gg = \left(\frac{\Delta_{Sc}^s + \Delta_{Sc}^{sd}}{\omega + \varepsilon_s(k)} \right) \left(\frac{1}{\omega - \varepsilon_s(k)} + \frac{\Delta_{Sc}^s + \Delta_{Sc}^{sd}}{\omega - \varepsilon_s(k)} \ll \hat{s}_{k\uparrow}^\dagger, \hat{s}_{-k\downarrow}^\dagger \gg \right), \quad (37)$$

$$\ll \hat{s}_{k\uparrow}^\dagger, \hat{s}_{-k\downarrow}^\dagger \gg = \frac{\Delta_{Sc}^s + \Delta_{Sc}^{sd}}{(\omega + \varepsilon_s(k))(\omega - \varepsilon_s(k))} + \left(\frac{\Delta_{Sc}^s + \Delta_{Sc}^{sd}}{\omega + \varepsilon_s(k)} \right) \times \left(\frac{\Delta_{Sc}^s + \Delta_{Sc}^{sd}}{\omega - \varepsilon_s(k)} \ll \hat{s}_{k\uparrow}^\dagger, \hat{s}_{-k\downarrow}^\dagger \gg \right), \quad (38)$$

$$\ll \hat{s}_{k\uparrow}^\dagger, \hat{s}_{-k\downarrow}^\dagger \gg = \frac{\Delta_{Sc}^s + \Delta_{Sc}^{sd}}{(\omega + \varepsilon_s(k))(\omega - \varepsilon_s(k))} + \frac{(\Delta_{Sc}^s + \Delta_{Sc}^{sd})^2}{(\omega + \varepsilon_s(k))(\omega - \varepsilon_s(k))} \ll \hat{s}_{k\uparrow}^\dagger, \hat{s}_{-k\downarrow}^\dagger \gg, \quad (39)$$

$$\left(1 - \frac{(\Delta_{Sc}^s + \Delta_{Sc}^{sd})^2}{(\omega + \varepsilon_s(k))(\omega - \varepsilon_s(k))} \right) \ll \hat{s}_{k\uparrow}^\dagger, \hat{s}_{-k\downarrow}^\dagger \gg = \frac{\Delta_{Sc}^s + \Delta_{Sc}^{sd}}{(\omega + \varepsilon_s(k))(\omega - \varepsilon_s(k))}, \quad (40)$$

$$\frac{(\omega + \varepsilon_s(k))(\omega - \varepsilon_s(k)) - (\Delta_{Sc}^s + \Delta_{Sc}^{sd})^2}{(\omega + \varepsilon_s(k))(\omega - \varepsilon_s(k))} \ll \hat{s}_{k\uparrow}^\dagger, \hat{s}_{-k\downarrow}^\dagger \gg = \frac{\Delta_{Sc}^s + \Delta_{Sc}^{sd}}{(\omega + \varepsilon_s(k))(\omega - \varepsilon_s(k))}, \quad (41)$$

$$\ll \hat{s}_{k\uparrow}^\dagger, \hat{s}_{-k\downarrow}^\dagger \gg = \frac{\Delta_{Sc}^s + \Delta_{Sc}^{sd}}{(\omega + \varepsilon_s(k))(\omega - \varepsilon_s(k)) - (\Delta_{Sc}^s + \Delta_{Sc}^{sd})^2}. \quad (42)$$

By ignoring Δ_{Sc}^{sd} , Eq. 42 reduces to the following.

$$\ll \hat{s}_{k\uparrow}^\dagger, \hat{s}_{-k\downarrow}^\dagger \gg = \frac{\Delta_{Sc}^s}{(\omega + \varepsilon_s(k))(\omega - \varepsilon_s(k)) - (\Delta_{Sc}^s)^2}. \quad (43)$$

By decoupling Eq. 43 using the partial fraction decomposition method, we have

$$\ll \hat{s}_{k\uparrow}^\dagger, \hat{s}_{-k\downarrow}^\dagger \gg = \frac{\Delta_{Sc}^s}{(\omega + \varepsilon_s(k))(\omega - \varepsilon_s(k)) - (\Delta_{Sc}^s)^2}, \quad (44)$$

$$\ll \hat{s}_{k\uparrow}^\dagger, \hat{s}_{-k\downarrow}^\dagger \gg = \frac{\Delta_{Sc}^s}{\omega^2 - \varepsilon_s^2(k) - (\Delta_{Sc}^s)^2}. \quad (45)$$

Using the expression $\omega \rightarrow i\omega_n$, where ω_n is the Matsubara frequency and written as

$$\omega_n = \frac{(2n+1)\pi}{\beta}, \quad (46)$$

$$\ll \hat{s}_{k\uparrow}^\dagger, \hat{s}_{-k\downarrow}^\dagger \gg = -\frac{\Delta_{Sc}^s}{\omega_n^2 - \varepsilon_s^2(k) - (\Delta_{Sc}^s)^2}, \quad (47)$$

$$\ll \hat{s}_{k\uparrow}^\dagger, \hat{s}_{-k\downarrow}^\dagger \gg = \frac{\Delta_{Sc}^s}{\omega_n^2 + \varepsilon_s^2(k) + (\Delta_{Sc}^s)^2}, \quad (48)$$

$$\ll \hat{s}_{k\uparrow}^\dagger, \hat{s}_{-k\downarrow}^\dagger \gg = \frac{\Delta_{Sc}^s}{\left(\frac{(2n+1)\pi}{\beta} \right)^2 + \varepsilon_s^2(k) + (\Delta_{Sc}^s)^2}, \quad (49)$$

$$\ll \hat{s}_{k\uparrow}^\dagger, \hat{s}_{-k\downarrow}^\dagger \gg = \frac{\beta^2 \Delta_{Sc}^s}{((2n+1)\pi)^2 + \beta^2 (\varepsilon_s^2(k) + (\Delta_{Sc}^s)^2)}. \quad (50)$$

Δ_{Sc}^s is written as

$$\Delta_{Sc}^s = \frac{U_s}{\beta} \sum_{k,n} \ll \hat{s}_{k\uparrow}^\dagger, \hat{s}_{-k\downarrow}^\dagger \gg. \quad (51)$$

Substituting Eq. 50 in Eq. 51, we have

$$\Delta_{Sc}^s = U_s \sum_{k,n} \frac{\beta \Delta_{Sc}^s}{((2n+1)\pi)^2 + \beta^2 (\varepsilon_s^2(k) + (\Delta_{Sc}^s)^2)}. \quad (52)$$

Let $\xi = \beta \sqrt{\varepsilon_s^2(k) + (\Delta_{Sc}^s)^2}$ and $\sum_{-\infty}^{\infty} \frac{1}{(2n+1)\pi^2 + \xi^2} = \frac{\tanh(\frac{\xi}{2})}{2\xi}$, then Eq. 52 can be written as

$$\Delta_{Sc}^s = \frac{U_s}{2} \sum_{k,n} \Delta_{Sc}^s 2\beta \frac{\tanh \frac{\xi}{2}}{\xi}. \quad (53)$$

Let us change summation into integration in the region $-\hbar\omega_F < \epsilon_s(k) < \hbar\omega_F$, and at the Fermi level, the density of state, $N_s(o)$, is

$$\sum_k \approx \int_{-\hbar\omega_F}^{\hbar\omega_F} N_s(o) d\epsilon_s(k), \tag{54}$$

$$\Delta_{Sc}^s = \frac{U_s}{2} \int_{-\hbar\omega_F}^{\hbar\omega_F} N_s(o) \Delta_{Sc}^s 2\beta \frac{\tanh \frac{\xi}{2}}{\xi} d\epsilon_s(k), \tag{55}$$

$$\frac{1}{U_s N_s(o)} = \int_0^{\hbar\omega_F} 2\beta \frac{\tanh \frac{\xi}{2}}{\xi} d\epsilon_s(k). \tag{56}$$

Let $\alpha = U_s N_s(o)$, which is called the superconducting coupling constant in the s-band intra-band interaction.

$$\frac{1}{\alpha} = \int_0^{\hbar\omega_F} \frac{\tanh\left(\frac{\beta}{2}(\epsilon_s^2(k) + (\Delta_{Sc}^s)^2)\right)}{(\epsilon_s^2(k) + (\Delta_{Sc}^s)^2)^{\frac{1}{2}}} d\epsilon_s(k). \tag{57}$$

Case I: If $T \rightarrow 0$, $\beta \rightarrow \infty$ this implies that $\tanh\left(\frac{\beta}{2}(\epsilon_s^2(k) + (\Delta_{Sc}^s)^2)\right) \rightarrow 1$

$$\frac{1}{\alpha} = \int_0^{\hbar\omega_F} \frac{1}{(\epsilon_s^2(k) + (\Delta_{Sc}^s)^2)^{\frac{1}{2}}} d\epsilon_s(k). \tag{58}$$

By applying the integral relation $\int \frac{1}{\sqrt{x^2+y^2}} dx = \ln(x + \sqrt{x^2+y^2})$, Eq. 58 gives

$$\frac{1}{\alpha} = \ln\left(\frac{\hbar\omega_F}{\Delta_{Sc}^s} + \left(\left(\frac{\hbar\omega_F}{\Delta_{Sc}^s}\right)^2 + 1\right)^{\frac{1}{2}}\right), \tag{59}$$

$$\frac{1}{\alpha} \approx \ln\left(2\frac{\hbar\omega_F}{\Delta_{Sc}^s}\right), \tag{60}$$

$$\Delta_{Sc}^s = 2\hbar\omega_F \exp\left(-\frac{1}{\alpha}\right). \tag{61}$$

From the concept of BCS theory, the superconducting order parameter Δ_{Sc}^s at $T = 0$ for a given superconductor with critical temperature T_c is written as $2\Delta_{Sc}^s(o) = 3.53K_B T_c$.

$$2\Delta_{Sc}^s(o) = 3.53K_B T_c = 4\hbar\omega_F \exp\left(-\frac{1}{\alpha}\right), \tag{62}$$

This gives

$$T_c = 1.14 \frac{\hbar\omega_F}{k_B} \exp\left(-\frac{1}{U_s N_s(o)}\right), \tag{63}$$

where $U_s = 0.323meV$, $N_s(o) = 1.5 (meV)^{-1}$, $k_B = 0.086 meV/K$ and $\hbar\omega_F = 6 meV$ [29]. Substituting these experimental values, we get $T_c = 10.09K$ that agrees with the experiment.

Case 2: If $0 < T < T_c$, then Eq. 57 is simplified as follows:

$$\frac{1}{\alpha} = 2\beta \int_0^{\hbar\omega_F} \sum_{-\infty}^{\infty} \frac{1}{((2n+1)\pi)^2 + \gamma^2} d\epsilon_s(k), \tag{64}$$

$$\frac{1}{\alpha} = \frac{2}{\beta} \int_0^{\hbar\omega_F} \sum_{-\infty}^{\infty} \frac{1}{\omega_n^2 + \epsilon_s^2(k) + (\Delta_{Sc}^s)^2} d\epsilon_s(k). \tag{65}$$

From the Laplacian transform with the Matsubara relation result, we can write Eq. 65 as

$$\frac{1}{\alpha} = \frac{2}{\beta} \int_0^{\hbar\omega_F} \sum_{-\infty}^{\infty} \frac{1}{\omega_n^2 + \epsilon_s^2(k)} d\epsilon_s(k) - (\Delta_{Sc}^s)^2 \frac{2}{\beta} \int_0^{\hbar\omega_F} \sum_{-\infty}^{\infty} \frac{1}{\omega_n^2 + \epsilon_s^2(k)} d\epsilon_s(k), \tag{66}$$

$$\frac{1}{\alpha} = 2\beta \int_0^{\hbar\omega_F} \sum_{-\infty}^{\infty} \frac{1}{(2n+1)^2 \pi^2 + (\beta \epsilon_s(k))^2} d\epsilon_s(k) - (\Delta_{Sc}^s)^2 \frac{2}{\beta} \int_0^{\hbar\omega_F} \sum_{-\infty}^{\infty} \frac{1}{(2n+1)^2 \left(\frac{\pi}{\beta}\right)^2 + \epsilon_s^2(k)} d\epsilon_s(k), \tag{67}$$

$$\frac{1}{\alpha} = \int_0^{\hbar\omega_F} \frac{\tanh\left(\frac{\beta}{2}\epsilon_s(k)\right)}{\epsilon_s^2(k)} d\epsilon_s(k) - 2(\Delta_{Sc}^s)^2 \frac{2}{\beta} \int_0^{\hbar\omega_F} \sum_0^{\infty} \frac{1}{(2n+1)^2 \left(\frac{\pi}{\beta}\right)^2 + \epsilon_s^2(k)} d\epsilon_s(k). \tag{68}$$

Applying the following equality $\sum_0^{\infty} \frac{1}{(y^2 + \epsilon_s^2(k))^2} d\epsilon_s(k) = 2 \sum_0^{\infty} \frac{1}{y^4(1+x^2)^2} d\epsilon_s(k)$ where $y^2 = (2n+1)^2 \left(\frac{\pi}{\beta}\right)^2$ and $x^2 = \frac{\epsilon_s^2(k)}{y^2}$.

$$\frac{1}{\alpha} = \int_0^{\hbar\omega_F} \frac{\tanh\left(\frac{\beta}{2}\epsilon_s(k)\right)}{\epsilon_s^2(k)} d\epsilon_s(k) - (\Delta_{Sc}^s)^2 \frac{4}{\beta} \int_0^{\hbar\omega_F} \sum_0^{\infty} \frac{1}{y^4(1+x^2)^2} d\epsilon_s(k). \tag{69}$$

From the above equality relations $x = \beta \frac{\epsilon_s(k)}{2}$ and $dx = \beta \frac{d\epsilon_s(k)}{2}$.

$$\frac{1}{\alpha} = \int_0^{\frac{\beta\hbar\omega_F}{2}} \frac{\tanh x}{x} dx - \frac{4}{\beta} \int_0^{\infty} \sum_0^{\infty} \frac{(\Delta_{Sc}^s)^2}{y^3(1+x^2)^2} dx, \tag{70}$$

$$= \ln\left(\frac{\beta\hbar\omega_F}{2}\right) \tanh\left(\frac{\beta\hbar\omega_F}{2}\right) - \int_0^{\frac{\beta\hbar\omega_F}{2}} \frac{\ln x}{\cosh^2 x} dx - \frac{4(\Delta_{Sc}^s)^2}{\beta y^3} \sum_0^{\infty} \int_0^{\infty} \frac{1}{(1+x^2)^2} dx, \tag{71}$$

$$= \ln\left(\frac{\beta\hbar\omega_F}{2}\right) \tanh\left(\frac{\beta\hbar\omega_F}{2}\right) - \ln\left(\frac{\pi}{4\gamma}\right) - \frac{4\beta^2 (\Delta_{Sc}^s)^2}{\pi^3} \sum_0^{\infty} \frac{1}{(2n+1)^3} \int_0^{\infty} \frac{1}{(1+x^2)^2} dx, \tag{72}$$

$$= \ln\left(\frac{\beta\hbar\omega_F}{2}\right) \tanh\left(\frac{\beta\hbar\omega_F}{2}\right) - \ln\left(\frac{\pi}{4\gamma}\right) - \frac{4\beta^2 (\Delta_{Sc}^s)^2}{\pi^3} \frac{7}{8} \xi(3) \frac{\pi}{4}. \tag{73}$$

For low temperature, $\tanh\left(\frac{\beta\hbar\omega_F}{2}\right) \rightarrow 1$ and γ denotes the Euler's constant, and its value is given by $\gamma = 1.78$. $\int_0^{\infty} \frac{1}{(1+x^2)^2} dx = \frac{\pi}{4}$ and $\sum_0^{\infty} \frac{1}{(2n+1)^3} = (1-2^{-3})\xi(3)$; this means $\xi(3) = 1.202$. So, after some steps, Eq. 73 can be written as

$$\frac{1}{\alpha} = \ln\left(1.14 \frac{\hbar\omega_F}{k_B T_c}\right) - 1.052 \left(\frac{\Delta_{Sc}^s}{\pi k_B T_c}\right)^2. \tag{74}$$

From Eq. 74, we have

$$\frac{1}{\alpha} = \ln\left(1.14 \frac{\hbar\omega_F}{k_B T_c}\right), \tag{75}$$

$$\ln\left(1.14 \frac{\hbar\omega_F}{k_B T_c}\right) = \ln\left(1.14 \frac{\hbar\omega_F}{k_B T_c}\right) - 1.052 \left(\frac{\Delta_{Sc}^s}{\pi k_B T_c}\right)^2, \tag{76}$$

$$\ln\left(1.14 \frac{\hbar\omega_F}{k_B T_c}\right) - \ln\left(1.14 \frac{\hbar\omega_F}{k_B T_c}\right) = -1.052 \left(\frac{\Delta_{Sc}^s}{\pi k_B T_c}\right)^2, \tag{77}$$

$$\ln\left(\frac{1.14 \frac{\hbar\omega_F}{k_B T_c}}{1.14 \frac{\hbar\omega_F}{k_B T_c}}\right) = -1.052 \left(\frac{\Delta_{Sc}^s}{\pi k_B T_c}\right)^2, \tag{78}$$

$$\ln\left(\frac{T}{T_c}\right) = -1.052 \left(\frac{\Delta_{Sc}^s}{\pi k_B T_c}\right)^2. \tag{79}$$

Using logarithmic series

$$\ln(\pm k) = \pm k - \frac{1}{2}k^2 \pm \frac{1}{3}k^3 - \dots$$

$$\ln\left(1 - \left(1 - \frac{T}{T_c}\right)\right) = -\left(1 - \frac{T}{T_c}\right) - \frac{1}{2}\left(\left(1 - \frac{T}{T_c}\right)\right)^2 - \frac{1}{3}\left(1 - \frac{T}{T_c}\right)^3 - \dots \tag{80}$$

Leaving the high-order terms, we get the following.

$$\ln\left(1 - \left(1 - \frac{T}{T_c}\right)\right) \approx -\left(1 - \frac{T}{T_c}\right), \tag{81}$$

$$-\left(1 - \frac{T}{T_c}\right) = -1.052\left(\frac{\Delta_{Sc}^s}{\pi k_B T_c}\right)^2, \tag{82}$$

$$1.052\left(\frac{\Delta_{Sc}^s}{\pi k_B T_c}\right) = \left(1 - \frac{T}{T_c}\right)^{\frac{1}{2}}, \tag{83}$$

$$\Delta_{Sc}^s = \frac{\pi}{1.025} k_B T_c \left(1 - \frac{T}{T_c}\right)^{\frac{1}{2}}, \tag{84}$$

$$\Delta_{Sc}^s(T) = 3.063 k_B T_c \left(1 - \frac{T}{T_c}\right)^{\frac{1}{2}}. \tag{85}$$

This equation tells us the superconducting order parameter Δ_{Sc}^s as a function of temperature. As temperature increases, the order parameter decrease and vanishes at T_c (10.09K). If T is zero, $\Delta_{Sc}^s = 2.658meV$.

2.1.2 Δ_{Sc}^d due to intra-band interactions within the d-band

Δ_{Sc}^d due to the intra-band interactions within the d band provided by

$$\Delta_{Sc}^d = \frac{U_s}{\beta} \sum_{k,n} \ll \hat{d}_{k\uparrow}^\dagger, \hat{d}_{-k\downarrow}^\dagger \gg. \tag{86}$$

By applying the same procedure as above, the superconducting transition temperature T_c due to the intra-band interactions within the d-band is written as

$$T_c = 1.14 \frac{\hbar\omega_F}{k_B} \exp\left(-\frac{1}{U_d N_d(o)}\right), \tag{87}$$

where $U_d = 0.267meV$, $N_d(o) = 1.80 (meV)^{-1}$, $k_B = 0.086 meV/K$ and $\hbar\omega_F = 6 meV$ [29]. Substituting these experimental values in this equation, we get $T_c = 9.92K$ that agrees with the experiment. The dependence of the superconducting order parameter Δ_{Sc}^d on temperature due to the intra-band interactions within the d-band is also given by

$$\Delta_{Sc}^d(T) = 3.063 k_B T_c \left(1 - \frac{T}{T_c}\right)^{\frac{1}{2}}. \tag{88}$$

Eq. 88 indicates the dependence of the superconducting order parameter on temperature in the d-band intra-band interaction in the pure superconducting region. The superconducting order parameter decreases as the temperature increases. It vanishes at T_c (9.92K). At $T = 0$, $\Delta_{Sc}^d = 2.163meV$.

2.1.3 Δ_{Sc}^{sd} due to the inter-band interaction between the s- and d-bands

The inter-band interaction between the s- and d-bands causes the superconducting order parameter, which can be connected to Green's function as

$$\Delta_{Sc}^{sd} = \frac{U_{sd}}{2} \sum_k \left(\ll \hat{s}_{k\uparrow}^\dagger, \hat{s}_{-k\downarrow}^\dagger \gg + \ll \hat{d}_{k\uparrow}^\dagger, \hat{d}_{-k\downarrow}^\dagger \gg \right) \tag{89}$$

Applying the same procedure, the equation of motion for the correlations $\ll \hat{s}_{k\uparrow}^\dagger, \hat{s}_{-k\downarrow}^\dagger \gg$ and $\ll \hat{d}_{k\uparrow}^\dagger, \hat{d}_{-k\downarrow}^\dagger \gg$ to describe the superconducting order parameter by using Green function formalism similar to the previous procedures due to the inter-band interaction is given by

$$\ll \hat{s}_{k\uparrow}^\dagger, \hat{s}_{-k\downarrow}^\dagger \gg = \frac{\Delta_{Sc}^s + \Delta_{Sc}^{sd}}{(\omega + \epsilon_s(k) - M)(\omega - \epsilon_s(k) + M) - (\Delta_{Sc}^s + \Delta_{Sc}^{sd})^2}$$

$$\text{and } \ll \hat{d}_{k\uparrow}^\dagger, \hat{d}_{-k\downarrow}^\dagger \gg = \frac{\Delta_{Sc}^d + \Delta_{Sc}^{sd}}{(\omega + \epsilon_d(k) - M)(\omega - \epsilon_d(k) + M) - (\Delta_{Sc}^d + \Delta_{Sc}^{sd})^2}.$$

Ignoring the intra-band superconducting order parameter terms and by decoupling these equations using the partial fraction decomposition method, we will have $\ll \hat{s}_{k\uparrow}^\dagger, \hat{s}_{-k\downarrow}^\dagger \gg = \frac{1}{2} \sum_{i=1}^2 \frac{\beta^2 \Delta_i(k)}{(2n+1)\pi^2 + \beta^2(\epsilon_s^2(k) + \Delta_i^2(k))}$ and $\ll \hat{d}_{k\uparrow}^\dagger, \hat{d}_{-k\downarrow}^\dagger \gg = \frac{1}{2} \sum_{i=1}^2 \frac{\beta^2 \Delta_i(k)}{(2n+1)\pi^2 + \beta^2(\epsilon_d^2(k) + \Delta_i^2(k))}$

where $\Delta_i(k) = \Delta_{Sc}^{sd} - 1(-1)^i M$, which is called the effective order parameter. Substituting these equations into Eq. 89, we get

$$\Delta_{Sc}^{sd} = \frac{U_{sd}}{2} \sum_k \left(\frac{1}{2} \sum_{i=1}^2 \frac{\beta^2 \Delta_i(k)}{((2n+1)\pi)^2 + \beta^2(\epsilon_s^2(k) + \Delta_i^2(k))} + \frac{U_{sd}}{2} \sum_k \left(\frac{1}{2} \sum_{i=1}^2 \frac{\beta^2 \Delta_i(k)}{((2n+1)\pi)^2 + \beta^2(\epsilon_d^2(k) + \Delta_i^2(k))} \right) \right). \tag{90}$$

Let $\epsilon_s(k) = \epsilon_d(k)$ in the inter-band interaction between the two bands, and Eq. 90 becomes

$$\Delta_{Sc}^{sd} = \frac{U_{sd}}{2} \sum_k \left(\frac{1}{2} \sum_{i=1,2} \frac{\beta^2 \Delta_i(k)}{((2n+1)\pi)^2 + \beta^2(\epsilon_s^2(k) + \Delta_i^2(k))} \right). \tag{91}$$

Let $\mu = \beta \sqrt{\epsilon_s^2(k) + \Delta_i^2(k)}$ and $\sum_{-\infty}^{\infty} \frac{1}{(2n+1)\pi^2 + \mu^2} = \frac{\tanh(\frac{\mu}{2})}{2\mu}$, then Eq. 91 is written as

$$\Delta_{Sc}^{sd} = \frac{U_{sd}}{4} \sum_{k,i=1,2} \Delta_i(k) \frac{\tanh \frac{\beta}{2} \sqrt{\epsilon_s^2(k) + \Delta_i^2(k)}}{\sqrt{\epsilon_s^2(k) + \Delta_i^2(k)}}. \tag{92}$$

Changing summation into integration in the region $-\hbar\omega_F < \epsilon_d(k) < \hbar\omega_F$, at the Fermi level, the density of state in the inter-band interaction is $N_{sd}(o)$, that is, $\sum_k \approx \int_{-\hbar\omega_F}^{\hbar\omega_F} N_{sd}(o) d\epsilon_s(k)$ The density of state $N_{sd}(o)$ is equal to $\sqrt{N_s(o)N_d(o)}$, then Eq. 92 becomes

$$\Delta_{Sc}^{sd} = \frac{U_{sd}}{4} \int_{-\hbar\omega_F}^{\hbar\omega_F} N_{sd}(o) \Delta_i(k) \frac{\tanh \frac{\beta}{2} \sqrt{\epsilon_s^2(k) + \Delta_i^2(k)}}{\sqrt{\epsilon_s^2(k) + \Delta_i^2(k)}} d\epsilon_s(k), \tag{93}$$

$$\frac{2}{U_{sd} \sqrt{N_s N_d(o)}} = \int_0^{\hbar\omega_F} \frac{\Delta_i(k)}{\Delta_{Sc}^{sd}} \frac{\tanh \frac{\beta}{2} \sqrt{\epsilon_s^2(k) + \Delta_i^2(k)}}{\sqrt{\epsilon_s^2(k) + \Delta_i^2(k)}} d\epsilon_s(k), \tag{94}$$

$$\frac{2}{U_{sd} \sqrt{N_s N_d(o)}} = \int_0^{\hbar\omega_F} \left(\frac{\Delta_{Sc}^{sd} - M}{\Delta_{Sc}^{sd}} \right) \frac{\tanh \frac{\beta}{2} \sqrt{\epsilon_s^2(k) + (\Delta_{Sc}^{sd} - M)^2}}{\sqrt{\epsilon_s^2(k) + (\Delta_{Sc}^{sd} - M)^2}} d\epsilon_s(k)$$

$$+ \int_0^{\hbar\omega_F} \left(\frac{\Delta_{Sc}^{sd} + M}{\Delta_{Sc}^{sd}} \right) \frac{\tanh \frac{\beta}{2} \sqrt{\epsilon_s^2(k) + (\Delta_{Sc}^{sd} + M)^2}}{\sqrt{\epsilon_s^2(k) + (\Delta_{Sc}^{sd} + M)^2}} d\epsilon_s(k). \tag{95}$$

After a couple of steps, the superconducting transition temperature T_c is given by

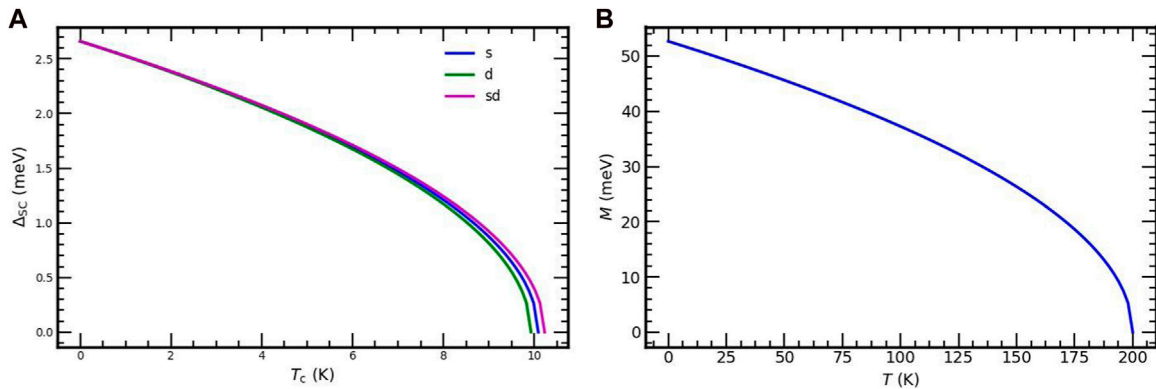


FIGURE 1 Superconducting order parameters vs. temperature for each interactions of the $SrFe_{2-x}Ni_xAs_2$ superconductor (A) and SDW order parameter (M) vs. temperature in the pure magnetic region of the $SrFe_{2-x}Ni_xAs_2$ superconductor (B).

$$T_c = 1.14 \frac{\hbar\omega_F}{k_B} \exp \left(-\frac{1}{U_{sd}\sqrt{N_s N_d(o)}} - \frac{M}{4K_B T_c} \ln \left(\frac{\hbar\omega_F + M}{\hbar\omega_F - M} \right) \right), \tag{96}$$

where $U_{sd} = 0.297\text{meV}$, $N_d(o) = 1.80\text{ (meV)}^{-1}$, $N_s(o) = 1.5\text{ (meV)}^{-1}$, $k_B = 0.086\text{ meV/K}$, and $\hbar\omega_F = 6\text{ meV}$ [29]. Eq. 96 clearly shows that the superconducting transition temperature depends on the SDW order parameter.

In the pure diamagnetism region $M = 0$, and Eq. 91 becomes $T_c = 1.14 \frac{\hbar\omega_F}{k_B} \exp \left(-\frac{1}{U_{sd}\sqrt{N_s N_d(o)}} \right)$ with $T_c = 10.20\text{K}$, which agrees with the experiment. For perfect diamagnetism, $M = 0$, and after some steps, the superconducting order parameter will be

$$\Delta_{SC}^{sd}(T) = 3.063k_B T_c \left(1 - \frac{T}{T_c} \right)^{\frac{1}{2}}. \tag{97}$$

This equation shows that the dependence of the superconducting order parameter on the temperature in the inter-band interactions between the s- and d-bands. The superconducting order parameter suppresses as the temperature increases. It vanishes at the superconducting transition temperature ($T_c = 10.20\text{K}$). If $T = 0$, $\Delta_{SC}^{sd}(0) = 2.687\text{meV}$.

2.2 SDW order parameter (M)

Using the double-time temperature-dependent Green's function to the equation of motion for the correlation $\ll \hat{s}_{-(k+p)\downarrow}, \hat{d}_{-k\downarrow}^\dagger \gg$, we will find the magnetic order parameter. To solve this problem, we start from the equation of motion for the correlation $\ll \hat{s}_{(k+p)\uparrow}^\dagger, \hat{d}_{-k\downarrow}^\dagger \gg$, and from double-time temperature-dependent Green's function, it can be described as

$$\omega \ll \hat{s}_{(k+p)\uparrow}^\dagger, \hat{d}_{-k\downarrow}^\dagger \gg = \left\langle \left[\hat{s}_{(k+p)\uparrow}^\dagger, \hat{d}_{-k\downarrow}^\dagger \right] \right\rangle + \ll \left[\hat{s}_{(k+p)\uparrow}^\dagger, \hat{H} \right], \hat{d}_{-k\downarrow}^\dagger \gg, \tag{98}$$

$$\omega \ll \hat{s}_{(k+p)\uparrow}^\dagger, \hat{d}_{-k\downarrow}^\dagger \gg = \left\langle \left[\hat{s}_{(k+p)\uparrow}^\dagger, \hat{d}_{-k\downarrow}^\dagger \right] \right\rangle + \ll \left[\hat{s}_{(k+p)\uparrow}^\dagger, \hat{H}_s + \hat{H}_d + \hat{H}_{sd} + \hat{H}_M \right], \hat{d}_{-k\downarrow}^\dagger \gg. \tag{99}$$

The commutation relations in Eq. 99 can be solved as follows:

$$\left[\hat{s}_{(k+p)\uparrow}^\dagger, \hat{H}_s \right] = -\epsilon_s(k+p) \hat{s}_{(k+p)\uparrow}^\dagger + \Delta_{SC}^s \hat{s}_{-(k+p)\downarrow}, \tag{100}$$

$$\left[\hat{s}_{(k+p)\uparrow}^\dagger, \hat{H}_d \right] = 0, \tag{101}$$

$$\left[\hat{s}_{(k+p)\uparrow}^\dagger, \hat{H}_{sd} \right] = \Delta_{SC}^{sd} \hat{s}_{-(k+p)\downarrow}, \tag{102}$$

$$\left[\hat{s}_{(k+p)\uparrow}^\dagger, \hat{H}_M \right] = M \hat{s}_{(k+p)\uparrow}^\dagger. \tag{103}$$

Substituting Eq. 100 to Eq. 103 in Eq. 99, it gives

$$\omega \ll \hat{s}_{(k+p)\uparrow}^\dagger, \hat{d}_{-k\downarrow}^\dagger \gg = \frac{\Delta_{SC}^s + \Delta_{SC}^{sd}}{\omega + \epsilon_s(k+p) - M} \ll \hat{s}_{-(k+p)\downarrow}, \hat{d}_{-k\downarrow}^\dagger \gg. \tag{104}$$

Now, let us find the equation of motion for the correlation $\ll \hat{s}_{-(k+p)\downarrow}, \hat{d}_{-k\downarrow}^\dagger \gg$ in Eq. 104.

$$\omega \ll \hat{s}_{-(k+p)\downarrow}, \hat{d}_{-k\downarrow}^\dagger \gg = 1 + \ll \left[\hat{s}_{-(k+p)\downarrow}, \hat{H}_s + \hat{H}_d + \hat{H}_{sd} + \hat{H}_M \right], \hat{d}_{-k\downarrow}^\dagger \gg. \tag{105}$$

Solving the commutation relations in Eq. 105, we get

$$\left[\hat{s}_{-(k+p)\downarrow}, \hat{H}_s \right] = \epsilon_s(k+p) \hat{s}_{-(k+p)\downarrow} + \Delta_{SC}^s \hat{s}_{(k+p)\uparrow}, \tag{106}$$

$$\left[\hat{s}_{-(k+p)\downarrow}, \hat{H}_d \right] = 0, \tag{107}$$

$$\left[\hat{s}_{-(k+p)\downarrow}, \hat{H}_{sd} \right] = \Delta_{SC}^{sd} \hat{s}_{(k+p)\uparrow}, \tag{108}$$

$$\left[\hat{s}_{-(k+p)\downarrow}, \hat{H}_M \right] = M \hat{s}_{-(k+p)\downarrow}. \tag{109}$$

Substituting Eq. 106 to Eq. 109 in Eq. 105, we get

$$\omega \ll \hat{s}_{-(k+p)\downarrow}, \hat{d}_{-k\downarrow}^\dagger \gg = \frac{1}{\omega - \epsilon(k+p) + M} + \frac{\Delta_{SC}^s + \Delta_{SC}^{sd}}{\omega - \epsilon(k+p) + M} \ll \hat{s}_{(k+p)\uparrow}^\dagger, \hat{d}_{-k\downarrow}^\dagger \gg. \tag{110}$$

Substituting Eq. 110 into Eq. 104 and after some mathematics, we get

TABLE 1 Superconducting transition temperature T_c values and the superconducting order parameter at $T = 0$ in different interactions for our compound $SrFe_{2-x}Ni_xAs_2$. The mean value of T_c is nearly 10K.

Interaction	Theoretical T_c value (K)	Δ_{Sc} at $T = 0$ (meV)
Intra-band interactions within the s -band	10.09	2.658
Intra-band interactions within the d -band	9.92	2.613
Inter-band interaction between the s - and d -bands	10.20	2.687

$$\langle\langle \hat{s}_{-(k+p)\uparrow} \hat{d}_{-k\downarrow}^\dagger \rangle\rangle = \frac{-\frac{1}{2}(\Delta_{Sc}^s + M)}{-\omega^2 + \epsilon_s^2(k+p) + (\Delta_{Sc}^s + M)^2} + \frac{\frac{1}{2}(\Delta_{Sc}^s - M)}{-\omega^2 + \epsilon_s^2(k+p) + (\Delta_{Sc}^s - M)^2}, \quad (111)$$

$$\frac{1}{UN(o)} = - \int_0^{\hbar\omega_F} \frac{\tanh\frac{\beta}{2}\sqrt{\epsilon_s^2(k) + M^2}}{\sqrt{\epsilon_s^2(k) + M^2}} d\epsilon_s(k). \quad (118)$$

where $\Delta_j(k) = \Delta_{Sc}^{sd} - 1(-1)^j M$, which is called the effective magnetic order parameter. Using the expression $\omega \rightarrow i\omega_n$ and applying the nesting condition, $\epsilon_s^2(k+p) = \epsilon_s^2(k)$. Eq. 111 gives

$$\langle\langle \hat{s}_{-(k+p)\uparrow} \hat{d}_{-k\downarrow}^\dagger \rangle\rangle = \frac{1}{2} \sum_{j=1,2} \frac{(-1)^j \Delta_j(k)}{\omega_n^2 + \epsilon_s^2(k) + \Delta_j^2(k)}. \quad (112)$$

The magnetic order parameter is given by

$$M = \frac{U}{\beta} \sum_k \langle\langle \hat{s}_{-(k+p)\uparrow} \hat{d}_{-k\downarrow}^\dagger \rangle\rangle. \quad (113)$$

Substituting Eq. 112 into Eq. 113; transforming summation into integration in the boundary $-\hbar\omega_F < \epsilon_s(k) < \hbar\omega_F$ and by presenting the density of state (DOS) at the Fermi level is $N(o)$, that is, $\sum_k \approx \int_{-\hbar\omega_F}^{\hbar\omega_F} N(o) d\epsilon_s(k)$, and after a couple of steps, we get

$$\frac{2}{UN(o)} = \frac{(-1)^j \Delta_j}{M} \int_0^{\hbar\omega_F} \frac{\tanh\frac{\beta}{2}\sqrt{\epsilon_s^2(k) + \Delta_i^2(k)}}{\sqrt{\epsilon_s^2(k) + \Delta_i^2(k)}} d\epsilon_s(k), \quad (114)$$

$$\frac{2}{UN(o)} = \frac{-(\Delta_{Sc}^s + M)}{M} \int_0^{\hbar\omega_F} \frac{\tanh\frac{\beta}{2}\sqrt{\epsilon_s^2(k) + (\Delta_{Sc}^s + M)^2}}{\sqrt{\epsilon_s^2(k) + (\Delta_{Sc}^s + M)^2}} d\epsilon_s(k) - \frac{(\Delta_{Sc}^s - M)}{M} \int_0^{\hbar\omega_F} \frac{\tanh\frac{\beta}{2}\sqrt{\epsilon_s^2(k) + (\Delta_{Sc}^s - M)^2}}{\sqrt{\epsilon_s^2(k) + (\Delta_{Sc}^s - M)^2}} d\epsilon_s(k). \quad (115)$$

After some steps, we get

$$\frac{1}{UN(o)} = \ln\left(1.14 \frac{\hbar\omega_F}{k_B T_M}\right) - 1.052 \left(\frac{M}{\pi k_B T_M}\right)^2 + \frac{\beta M}{4} \ln\left(\frac{\hbar\omega_F + M}{\hbar\omega_F - M}\right). \quad (116)$$

For small values of M , we ignore the M^2 term. Thus, Eq. 116 reduces to

$$T_M = 1.14 \frac{\hbar\omega_F}{k_B} \exp\left(-\frac{1}{UN(o)} + \frac{\beta M}{4} \ln\left(\frac{\hbar\omega_F + M}{\hbar\omega_F - M}\right)\right), \quad (117)$$

where $UN(o) = 1.68$ [29] and it is the SDW coupling parameter. Eq. 117 shows that the SDW order parameter increases as the SDW transition temperature increases.

For the pure magnetic region $\Delta_{Sc}^s = 0$ and Eq. 115 becomes

This is simplified to

$$-\frac{1}{UN(o)} = \ln\left(1.14 \frac{\hbar\omega_F}{k_B T}\right) - 1.052 \left(\frac{M}{\pi k_B T}\right)^2. \quad (119)$$

For a little value of M , $M^2 \rightarrow 0$ and $T \rightarrow T_M$. Eq. 119 reduces

$$-\frac{1}{UN(o)} = \ln\left(1.14 \frac{\hbar\omega_F}{k_B T_M}\right). \quad (120)$$

This implies that

$$\ln\left(1.14 \frac{\hbar\omega_F}{k_B T_M}\right) = \ln\left(1.14 \frac{\hbar\omega_F}{k_B T}\right) - 1.052 \left(\frac{M}{\pi k_B T_M}\right)^2. \quad (121)$$

Eq. 121 simplifies to

$$M = \frac{\pi k_B T_M}{1.052} \left(1 - \frac{T}{T_M}\right)^{\frac{1}{2}}, \quad (122)$$

$$M(T) = 3.063 k_B T_M \left(1 - \frac{T}{T_M}\right)^{\frac{1}{2}}. \quad (123)$$

Eq. 123 indicates that if temperature rises, the SDW order parameter suppresses.

3 Results and discussion

In this part, we discussed how temperature (T) affects superconducting order parameters (Δ_{Sc}) and the SDW order parameter (M), and M affects on both the SDW transition temperature (T_M) and superconducting transition temperature (T_c). We expand on the analysis. In a two-band model for $SrFe_{2-x}Ni_xAs_2$, we created the theoretical examination of the coexistence of superconductivity and SDW. With the aid of a two-band Hamiltonian model and the double-time temperature-dependent Green's function formal consideration, we were able to derive the mathematical expressions for the superconducting transition temperature (T_c), superconducting order parameters for each intra- and inter-band interactions, SDW order parameter (M), and SDW transition temperature (T_M).

From Eqs 63, 87, 96, we obtain the superconducting transition (critical) temperatures for each intra- and inter-band interactions of $SrFe_{2-x}Ni_xAs_2$. Using these (T_c) values and Eqs 85, 88, 97, respectively, we plotted the phase diagram of Δ_{Sc} versus T within each intra-band and inter-band interactions, Figure 1A.

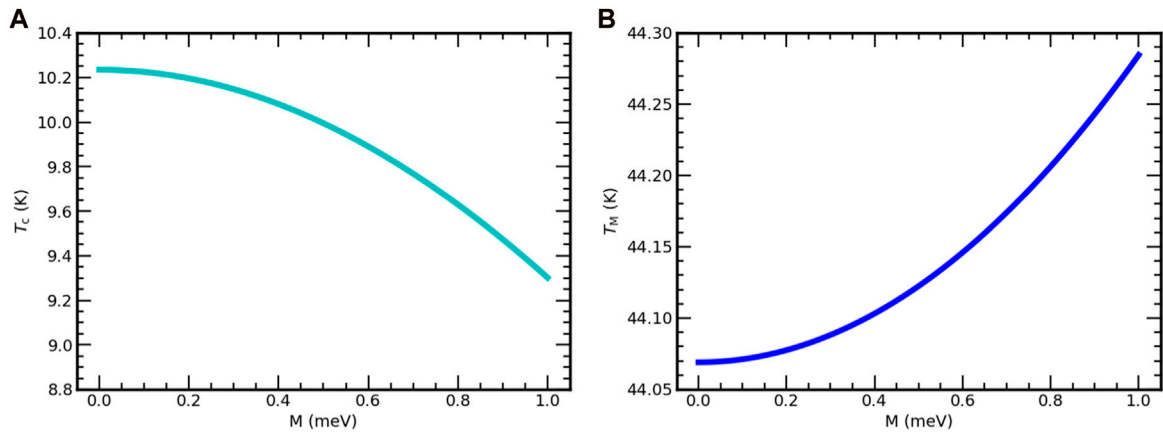


FIGURE 2 Superconducting transition temperature (T_c) versus the SDW order parameter (M) for the inter-band interaction of the $SrFe_{2-x}Ni_xAs_2$ superconductor (A) and SDW transition temperature (T_M) versus SDW order parameter (M) of $SrFe_{2-x}Ni_xAs_2$ (B).

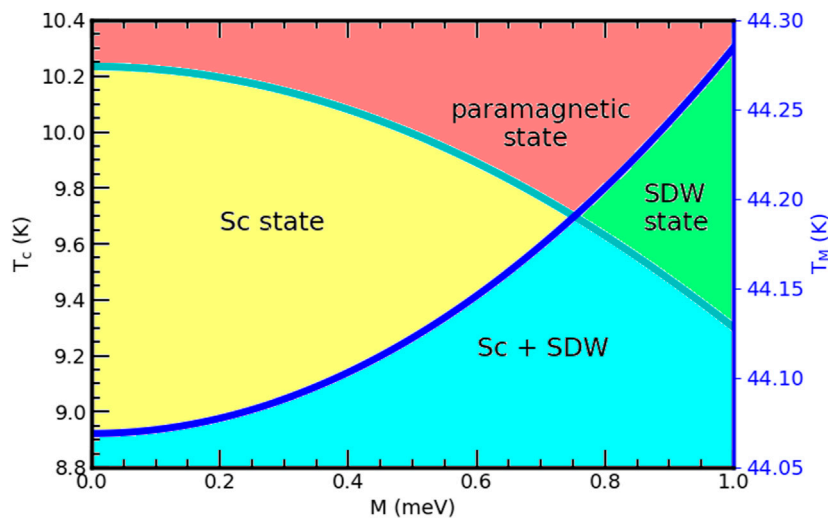


FIGURE 3 Superconducting critical temperature and magnetic transition temperature vs. the SDW order parameter for the $SrFe_{2-x}Ni_xAs_2$ superconductor.

As illustrated in Figure 1A, the superconducting order parameter decreases as the temperature increases. It vanishes as the temperature is equal to the critical temperature. For the s intra-band interaction, the maximum value of the superconducting order parameter, $(\Delta_{Sc}^s) = 2.658 \text{ meV}$, occurs at $T = 0$, and it vanishes at the superconducting transition temperature $T_c = 10.09\text{K}$. For the d intra-band interaction, the maximum value of the superconducting order parameter, $\Delta_{Sc}^d = 2.613 \text{ meV}$, occurs at $T = 0$, and $\Delta_{Sc}^d = 0$ at the superconducting transition temperature $T_c = 9.92\text{K}$. Moreover, $\Delta_{Sc}^{sd} = 2.687\text{meV}$ at $T = 0$ and $\Delta_{Sc}^{sd} = 0$ at the superconducting transition temperature $T_c = 10.20\text{K}$ for the inter-band interaction. For each intra-band and inter-band interactions of the $SrFe_{2-x}Ni_xAs_2$ superconductor, the theoretical values of superconducting transition temperatures agree with the

experimental value, which is around $T_c = 10\text{K}$, as discussed in Table 1 [34].

Based on Eq. 123, we plotted the phase illustration for the dependence of the magnetic order parameter (M) on temperature in the pure magnetic region illustrated in Figure 1B. As illustrates from this figure, magnetism decreases as the temperature enhances and vanishes at the SDW transition temperature $T_M = 205\text{K}$. The maximum value of the SDW order parameter, $M = 54 \text{ meV}$, occurs at $T = 0$. This finding is also in agreement with experimental observations [34, 37].

Based on Eq. 96, we plotted the phase diagrams of T_c versus M . As illustrated from Figure 2A, when the value of the SDW order parameter enhances, the superconducting transition temperature is suppressed for $SrFe_{2-x}Ni_xAs_2$. From this figure, one can see the SDW

order parameter promotes the magnetic nature and suppresses superconductivity in the system.

Using Eq. 117, we also plotted the phase plotting of the SDW transition temperature (T_M) versus the SDW order parameter (M), as seen in Figure 2B. As demonstrated from this figure, (T_M) progressively gets bigger with the SDW order parameter of the $SrFe_{2-x}Ni_xAs_2$ superconductor.

Finally, by combining Figures 2A, B, this article depicted a region where both SDW and superconductivity coexist, as shown in Figure 3. Because of their coexistence, the iterating superconducting electrons and spins are thought to have a weak exchange coupling for $SrFe_{2-x}Ni_xAs_2$. This figure shows that the possible interplay of superconductivity and SDW for $SrFe_{2-x}Ni_xAs_2$. As indicated in this figure, our finding is in agreement with experimental observations [34, 37]. This figure also depicts there are regions that show the superconducting and anti-ferromagnetic states segregate, which indicates that there are regions where magnetic and superconducting phases are not mixed.

4 Conclusion

In this work, we have studied the possibility of coexisting superconductivity and magnetism for the iron-based superconductor $SrFe_{2-x}Ni_xAs_2$. The superconductivity order parameter for $SrFe_{2-x}Ni_xAs_2$ is suppressed as the temperature raises and vanishes at the superconducting critical temperature. The magnitude of the SDW order parameter for $SrFe_{2-x}Ni_xAs_2$ is suppressed as the superconducting critical temperature increases and increases with increasing the SDW transition temperature. We depicted the possibility of coexisting superconductivity and magnetism in the $SrFe_{2-x}Ni_xAs_2$ superconductor. For the iron-based superconductor $SrFe_{2-x}Ni_xAs_2$, we further studied the reliance of the SDW order

parameter M on temperature in the pure magnetic region. When temperature increases, the SDW order parameter is suppressed and is zero at the SDW transition temperature of the $SrFe_{2-x}Ni_xAs_2$ superconductor.

Data availability statement

The raw data supporting the conclusion of this article will be made available by the authors, without undue reservation.

Author contributions

All authors listed have made a substantial, direct, and intellectual contribution to the work and approved it for publication.

Conflict of interest

The authors declare that the research was conducted in the absence of any commercial or financial relationships that could be construed as a potential conflict of interest.

Publisher's note

All claims expressed in this article are solely those of the authors and do not necessarily represent those of their affiliated organizations, or those of the publisher, the editors, and the reviewers. Any product that may be evaluated in this article, or claim that may be made by its manufacturer, is not guaranteed or endorsed by the publisher.

References

- John R. *Solid state physics* 1st ed. India: New Delhi McGraw-Hill Education (2014). p. 24. 110016.
- Kim CJ, Kim CJ. *History of superconductivity* Singapore. Superconductor Levitation: Concepts and Experiments (2019). p. 1–11. doi:10.1007/978-981-13-6768-7_1
- Raychaudhuri P, Dutta S. Phase fluctuations in conventional superconductors. *J Phys Condensed Matter* (2021) 34(8):083001. doi:10.1088/1361-648X/ac360b
- Zhu Z, Papaj M, Nie XA, Xu HK, Gu YS, Yang X, et al. Discovery of segmented Fermi surface induced by Cooper pair momentum. *Science* (2021) 374(6573):1381–5. doi:10.1126/science.abf1077
- Qiu D, Gong C, Wang S, Zhang M, Yang C, Wang X, et al. Recent advances in 2D superconductors. *Adv Mater* (2021) 33(18):2006124. doi:10.1002/adma.202006124
- Naqib SH, Islam RS. Possible quantum critical behavior revealed by the critical current density of hole doped high-T c cuprates in comparison to heavy fermion superconductors. *Scientific Rep* (2019) 9(1):14856. doi:10.1038/s41598-019-51467-4
- Bussmann-Holder A, Keller H. High-temperature superconductors: underlying physics and applications. *Z für Naturforschung B* (2020) 75(1-2):3–14. doi:10.1515/znb-2019-0103
- Maksimovic N. *Advances in nearly-magnetic superconductivity*. Berkeley: University of California (2022).
- Li H. *Spectroscopic-imaging scanning tunneling microscopy studies on cuprates high temperature superconductors*. United States: Stony Brook Doctoral dissertation, State University of New York at Stony Brook (2021).
- Rasaki SA, Thomas T, Yang M. Iron based chalcogenide and pnictide superconductors: from discovery to chemical ways forward. *Prog Solid State Chem* (2020) 59:100282. doi:10.1016/j.progsolidchem.2020.100282
- Carretta P, Prando G. Iron-based superconductors: tales from the nuclei. *La Rivista Del Nuovo Cimento* (2020) 43(1):1–43. doi:10.1007/s40766-019-0001-1
- Fernandes RM, Coldea AI, Ding H, Fisher IR, Hirschfeld PJ, Kotliar G. Iron pnictides and chalcogenides: a new paradigm for superconductivity. *Nature* (2022) 601(7891):35–44. doi:10.1038/s41586-021-04073-2
- Kreisler A, Hirschfeld PJ, Andersen BM. On the remarkable superconductivity of FeSe and its close cousins. *Symmetry* (2020) 12(9):1402. doi:10.3390/sym12091402
- Roter B, Ninkovic N, Dordevic SV. Clustering superconductors using unsupervised machine learning. *Physica C: Superconductivity its Appl* (2022) 598:1354078. doi:10.1016/j.physc.2022.1354078
- Kim TK, Pervakov KS, Evtushinsky DV, Jung SW, Poelchen G, Kummer K, et al. Electronic structure and coexistence of superconductivity with magnetism in $RbEuFe_4As_4$. *Phys Rev B* (2021) 103(17):174517. doi:10.1103/PhysRevB.103.174517
- Yu AB, Huang Z, Zhang C, Wu YF, Wang T, Xie T, et al. Superconducting anisotropy and vortex pinning in $CaKFe_4As_4$ and $KCa_2Fe_4As_4F_2$. *Chin Phys B* (2021) 30(2):027401. doi:10.1088/1674-1056/abc988
- Park JT, Friemel G, Li Y, Kim JH, Tsurkan V, Deisenhofer J, et al. Magnetic resonant mode in the low energy spin-excitation spectrum of superconducting $Rb_2Fe_4Se_5$ single crystals. *Phys Rev Lett* (2011) 107(17):177005. doi:10.1103/physrevlett.107.177005
- Charnukha A, Cvitkovic A, Prokscha T, Propper D, Ocelic N, Suter A, et al. Nanoscale layering of antiferromagnetic and superconducting phases in $Rb_2Fe_4Se_5$ single crystals. *Phys Rev Lett* (2012) 109(1):017003. doi:10.1103/PhysRevLett.109.017003
- Gui X, Lv B, Xie W. Chemistry in superconductors. *Chem Rev* (2021) 121(5):2966–91. doi:10.1021/acs.chemrev.0c00934

20. Bogale GM, Shiferaw DA. *High entropy materials-microstructures and properties" in iron-based superconductors*. Rijeka: Croatia IntechOpen (2022). p. 1–19. doi:10.5772/intechopen.109045
21. Ma X, Wang G, Liu R, Yu T, Peng Y, Zheng P, et al. Correlation-corrected band topology and topological surface states in iron-based superconductors. *Phys Rev B* (2022) 106(11):115114. doi:10.1103/PhysRevB.106.115114
22. Tam DW, Berlijn T, Maier TA. Stabilization of s-wave superconductivity through arsenic p-orbital hybridization in electron-doped BaFe₂As₂. *Phys Rev B* (2018) 98(2):024507. doi:10.1103/PhysRevB.98.024507
23. Zhang R. *Neutron scattering studies of the magnetic excitations in 122 family of iron pnictides (doctoral dissertation)*. Houston: Texas Rice University (2022).
24. Christensen MH, Kang J, Fernandes RM. Intertwined spin-orbital coupled orders in the iron-based superconductors. *Phys Rev B* (2019) 100(1):014512. doi:10.1103/PhysRevB.100.014512
25. Gruner G. *Density waves in solids*. Boca Raton: Florida CRC Press (2018). doi:10.1201/9780429501012
26. Kokanova SV, Maksimov PA, Rozhkov AV, Sboychakov AO. Competition of spatially inhomogeneous phases in systems with nesting-driven spin-density wave state. *Phys Rev B* (2021) 104(7):075110. doi:10.1103/PhysRevB.104.075110
27. Araujo RDMT, Zarpellon J, Mosca DH. Unveiling ferromagnetism and antiferromagnetism in two dimensions at room temperature. *J Phys D: Appl Phys* (2022) 55(28):283003. doi:10.1088/1361-6463/ac60cd
28. Ali K, Adhikary G, Thakur S, Patil S, Mahatha SK, Thamizhavel A, et al. Hidden phase in parent Fe-pnictide superconductors. *Phys Rev B* (2018) 97(5):054505. doi:10.1103/PhysRevB.97.054505
29. Chen X, Liu N, Guo J, Chen X. Direct response of the spin-density wave transition and superconductivity to anion height in SrFe₂As₂. *Phys Rev B* (2017) 96(13):134519. doi:10.1103/PhysRevB.96.134519
30. Gati E, Xiang L, Bud'ko SL, Canfield PC. Hydrostatic and uniaxial pressure tuning of iron-based superconductors: insights into superconductivity, magnetism, nematicity, and collapsed tetragonal transitions. *Annalen der Physik* (2020) 532(10):2000248. doi:10.1002/andp.202000248
31. Wu JJ, Lin JF, Wang XC, Liu QQ, Zhu JL, Xiao YM, et al. Pressure-decoupled magnetic and structural transitions of the parent compound of iron-based 122 superconductors BaFe₂As₂. *Proc Natl Acad Sci* (2013) 110(43):17263–6. doi:10.1073/pnas.1310286110
32. Chong SV, Tallon JL, Fang F, Kennedy J, Kadowaki K, Williams GVM. Surface superconductivity on SrFe₂As₂ single crystals induced by ion implantation. *EPL (Europhysics Letters)* (2011) 94(3):37009. doi:10.1209/0295-5075/94/37009
33. Hosono H, Fukuyama H, Akai H. Iron-based superconductors. *Handbook Superconductivity: Fundamentals Mater One* (2022) 1:293–301. doi:10.1201/9780429179181-30
34. Butch NP, Saha SR, Zhang XH, Kirshenbaum K, Greene RL, Paglione J. Effective carrier type and field dependence of the reduced-T_c superconducting state in SrFe_{2-x}Ni_xAs₂. *Phys Rev B* (2010) 81(2):024518. doi:10.1103/PhysRevB.81.024518
35. Saha SR, Butch NP, Kirshenbaum K, Paglione J. Annealing effects on superconductivity in SrFe_{2-x}Ni_xAs₂. *Physica C, Superconductivity* (2010) 470: S379–81. doi:10.1016/j.physc.2009.11.079
36. Xie T, Gong D, Ghosh H, Ghosh A, Soda M, Masuda T, et al. Neutron spin resonance in the 112-type iron-based superconductor. *Phys Rev Lett* (2018) 120(13):137001. doi:10.1103/PhysRevLett.120.137001
37. Saha SR, Butch NP, Kirshenbaum K, Paglione J. Evolution of bulk superconductivity in SrFe₂As₂ with Ni substitution. *Phys Rev B* (2009) 79(22):224519. doi:10.1103/PhysRevB.79.224519
38. Yao C, Ma Y. Superconducting materials: challenges and opportunities for large-scale applications. *Iscience* (2021) 24(6):102541. doi:10.1016/j.isci.2021.102541
39. Kidanemariam T, Khasay G, Mebrahtu A. Theoretical investigation of the coexistence of superconductivity and spin density wave (SDW) in two-band model for the iron-based superconductor BaFe₂(As_{1-x}P_x)₂. *The Eur Phys J B* (2019) 92(2):39–12. doi:10.1140/epjb/e2019-80638-9
40. Han Q, Chen Y, Wang ZD. A generic two-band model for unconventional superconductivity and spin-density-wave order in electron- and hole-doped iron-based superconductors. *EPL (Europhysics Letters)* (2008) 82(3):37007. doi:10.1209/0295-5075/82/37007
41. Mebratie G, Bekele T. Theoretical investigation of the interplay of superconductivity and magnetism in Ba_{1-x}K_xFe₂As₂ superconductor in a two-band model by using the bogoliubov transformation formalism. *Adv Condensed Matter Phys* (2023) 2023:1–14. doi:10.1155/2023/9556764